

Derivation and numerical approximation of hyperbolic viscoelastic flow systems: Saint-Venant 2D equations for Maxwell fluids

Sébastien Boyaval, Laboratoire d'hydraulique Saint-Venant
(EDF R&D – Ecole des Ponts ParisTech – CEREMA) Université Paris-Est
EDF'lab 6 quai Watier 78401 Chatou Cedex France,
& INRIA Paris, MATHERIALS (sebastien.boyaval@enpc.fr)

December 12, 2017

Abstract

We pursue here the development of models for complex (viscoelastic) fluids in *shallow free-surface gravity flows* which was initiated by [Bouchut-Boyaval, M3AS (23) 2013] for 1D (translation invariant) cases.

The models we propose are *hyperbolic* quasilinear systems that generalize Saint-Venant shallow-water equations to incompressible *Maxwell fluids*. The models are compatible with a formulation of the thermodynamics second principle. In comparison with Saint-Venant standard shallow-water model, the momentum balance includes extra-stresses associated with an elastic potential energy in addition to a hydrostatic pressure. The extra-stresses are determined by an additional tensor variable solution to a differential equation with various possible time rates.

For the numerical evaluation of solutions to Cauchy problems, we also propose *explicit* schemes discretizing our generalized Saint-Venant systems with Finite-Volume approximations that are *entropy-consistent* (under a CFL constraint) in addition to satisfy exact (discrete) mass and momentum conservation laws. In comparison with most standard viscoelastic numerical models, our discrete models can be used for any retardation-time values (i.e. in the vanishing “solvent-viscosity” limit).

We finally illustrate our hyperbolic viscoelastic flow models numerically using computer simulations in benchmark test cases. On extending to Maxwell fluids some free-shear flow testcases that are standard benchmarks for Newtonian fluids, we first show that our (numerical) models reproduce well the viscoelastic physics, phenomenologically at least, with zero retardation-time. Moreover, with a view to quantitative evaluations, numerical results in the lid-driven cavity testcase show that, in fact, our models can be compared with standard viscoelastic flow models in sheared-flow benchmarks on adequately choosing the physical parameters of our models. Analyzing our models asymptotics should therefore shed new light on the famous High-Weissenberg Number Problem (HWNP), which is a limit for all the existing viscoelastic numerical models.

1 Introduction

Modelling the viscoelastic large deformation of a flowing continuum material is still a challenge, despite more than a century of attempts after Maxwell [32]. Precisely, to numerically predict the evolution in time of realistic non-Newtonian *fluid* continuum materials, one does not know yet a good mathematical model for Eulerian fields characterizing a multidimensional flow that would properly generalize Maxwell’s one-dimensional (1D) model.

In addition to respect the fundamental physical principles (Galilean invariance, mass conservation etc.), a good viscoelastic model should account i) for the stresses generated within the fluid by a loss of elastic (potential) energy in deformations – shear and extension –, and ii) for the (viscous) energy dissipation leading the fluid to a flow equilibrium.

Many *constitutive equations* have been proposed to relate the stresses with the symmetrized velocity gradient as a measure of strain, which are formally satisfying from the loose viewpoint above, but research is still going on [8]. Indeed, there seems to be no general model yet that allows one to correctly match the experimentally-observed behaviour of complex fluids in steady flows, like shear-thinning and strain-hardening, see e.g. [7, 39].

Moreover, in any case, a good model should also allow one to predict the evolution in time of a piece of fluid, at least for small times, knowing initial conditions (a Cauchy initial-value problem). Now, most numerical viscoelastic flow model use similar sets of PDEs for a mass density ρ , a *solenoidal* velocity \mathbf{u} , and a 2-tensor $\mathbf{\Sigma}$ with various possible physical interpretations with the Eulerian viewpoint. Typically, differential models of *rate-type* have been proposed for Maxwell fluids when the tensor field $\mathbf{\Sigma}$ is either Cauchy’s stress tensor or a strain tensor like Cauchy-Green, see e.g. [33, 7, 39]. But despite some recent mathematical progress showing that Cauchy problems for physically-interesting models like FENE-P and Giesekus have global solutions [31], the *numerical computation* of solutions remains unsatisfying too.

There has been continuing progress in the numerical discretization of Cauchy problems for viscoelastic models [35, 19, 36, 1, 28, 41] and its analysis [13, 2, 37, 4]. However, numerical computations remain impossible in some physically-meaningful configurations at moderately high Weissenberg number in particular, which is quite frustrating for applications.

We note that all the discrete viscoelastic models mentioned above consider the *solenoidal* flows of incompressible Maxwell fluids, with a non-zero *retardation time* (i.e. they have a “background” viscous stress term justified by the *solvent viscosity* in the context of polymer flows). Then, they rely on the assumption that velocity gradients remain bounded, and numerical *steady-state flows* are usually computed using iterative algorithms to approximate the nonlinear terms (of the constitutive equations at least). Now, numerical instabilities typically occur when the nonlinear terms prevail in the (discrete) equations and iterative algorithms fail to converge (to an implicit time-discretization e.g.).

In this work, we would like to study discrete viscoelastic models that are explicitly computable (no iterative algorithm is required for the approximation of nonlinearities as fixed points) and that do not assume a non-zero retardation time (velocity gradients are possibly undounded). Hence, we consider quasilinear systems of first-order with possibly non-solenoidal velocities, that express mass and energy conservation for elastic fluids with one single relaxation time

(so-called Maxwell fluids). Moreover, for the sake of stability, we consider hyperbolic systems endowed with an additional conservation law (in smooth evolutions) as a formulation of the second thermodynamics principle. Even if one single additional conservation law may not suffice to define *unique* admissible solutions to multidimensional hyperbolic systems, see e.g. [15], it can be useful for numerical stability purposes at least, see e.g. [13, 2, 37, 4].

A quasilinear system of PDEs has been considered as a model for viscoelastic 2D flows of a slightly compressible Maxwell fluid in [38, 18, 25, 24]. It uses the Upper-Convected Maxwell equation for the stress tensor Σ (like Oldroyd-B model) and it is hyperbolic under a simple physically-natural condition *that is independent of the system parameters* when rewritten in terms of a deformation tensor (the left Cauchy-Green deformation tensor, see below in Section 2.1). Numerical computations show the interest of the approach. However, the model does not conserve mass and is not obviously compatible with thermodynamics principles. Moreover, it does not seem easily generalized to 3D flows, and its stress-strain relationship is physically unclear.

In this work, we use the simplified Saint-Venant framework for hydrostatic 2D (shallow) free-surface flows to propose and study quasilinear systems such that: (i) they model incompressible viscoelastic flows of Maxwell fluids with a *deformation tensor* as dependent variable, (ii) they conserve mass and satisfy a formulation of the thermodynamics principles, (iii) they remain hyperbolic under simple physically-natural admissibility conditions. Two possible models are identified in Section 2.

One model uses the Upper-Convected Maxwell equation for a deformation tensor of Cauchy-Green left type. It is very similar to that in [38, 18, 25, 24] except that it is rewritten in terms of a deformation tensor (which then allows us to show why it is hyperbolic under a condition independent of the system parameters). In comparison, our version additionally conserves mass (to that aim, we introduce a free-surface and decompose the pressure in two terms) and it is endowed with a formulation of the thermodynamics principles. This is one of the 2D models for viscoelastic incompressible shallow free-surface flows under gravity that generalize Saint-Venant's approach (initially for shallow *water*) to non-Newtonian fluids, which we previously derived in [11] after depth-averaging Oldroyd-B model for fast thin-layer flows with small viscosity.

Another model is proposed that uses *Finger* deformation tensor (the *inverse* of Cauchy-Green left one), with a clear stress-strain relationship (using Euler-Almansi strain) and with *Cotter-Rivlin* natural frame-invariant time-rate-of-change. The model is hyperbolic under the same simple physically-natural conditions as the previous one, it conserves mass, and it is endowed with a similar formulation of the thermodynamics principles. We also note that the model is similar to Reynolds-averaged models that have been proposed for the Reynolds stresses in weakly-sheared turbulent flows [45, 44], see also [26].

In Section 3, we propose entropy-consistent Finite-Volume discretizations of the two models. The numerical scheme is a 2D extension of the Suliciu-type relaxation approach developed in [10] for a closed subsystem fully describing the 1D (translation-invariant) motions (see also [12] for the exact solutions to the 1D Riemann problems).

In Section 4, we perform numerical simulations. The numerical results show that our model are physically meaningful, and a viable approach to the computer

simulation of physically-realistic viscoelastic flows.

2 Hyperbolic viscoelastic Saint-Venant systems

2.1 Saint-Venant models for shallow free-surface flows

Given a constant gravity field $\mathbf{g} = -g\mathbf{e}_z$, let us equip space with a Cartesian frame $(\mathbf{e}_x, \mathbf{e}_y, \mathbf{e}_z)$ and consider the flow, i.e. the evolution in time and space, of a viscoelastic fluid material with a non-folded free-surface $z = H(t, x, y) \geq 0$ above a flat impermeable plane $z = 0$. We assume the fluid material incompressible with constant mass density. Then, the dynamics of the flow is governed by a kinematic condition for the free-surface (in virtue of the mass conservation principle) coupled to a momentum-balance equation for the velocity (u, v, w) following physical principles.

Assuming the flow *stratified* (i.e. with the acceleration small in vertical direction, and with the horizontal components (u, v) of the velocity mostly uniform in vertical direction) such that

$$H \int_0^H dz u^2 \approx \left(\int_0^H dz u \right)^2 \quad H \int_0^H dz v^2 \approx \left(\int_0^H dz v \right)^2$$

one standardly obtains an interesting system of quasilinear equations for $H > 0$ and the depth-averaged velocity $\mathbf{U} = (U, V)$ with components $U \approx \frac{1}{H} \int_0^H dz u$, $V \approx \frac{1}{H} \int_0^H dz v$ in the form of conservation laws:

$$\partial_t H + \operatorname{div}(H\mathbf{U}) = 0 \tag{1}$$

$$\partial_t(H\mathbf{U}) + \operatorname{div}(H\mathbf{U} \otimes \mathbf{U} + H(P + \Sigma_{zz})\mathbf{I} - H\Sigma_h) = -kH\mathbf{U} \tag{2}$$

equivalently:

$$\partial_t H + \partial_x(HU) + \partial_y(HV) = 0$$

$$\partial_t(HU) + \partial_x(HUU + HP + H\Sigma_{zz} - H\Sigma_{xx}) + \partial_y(HUV - H\Sigma_{xy}) = -kHU$$

$$\partial_t(HV) + \partial_x(HUV - H\Sigma_{yx}) + \partial_y(HVV + HP + H\Sigma_{zz} - H\Sigma_{yy}) = -kHV$$

which is reminiscent of the 2D gas-dynamics equations of Euler with mass density proportional to H , with *specific* pressure $P + \Sigma_{zz}$ and with *specific* stress-deviator Σ_h . (P and Σ_{ij} have the dimension of energy per unit mass rather than per unit volume, unlike standard Cauchy stresses and pressures typically measured in Pa, that is why we term them *specific*. But for the sake of simplicity, we omit the label “specific” below, insofar as this is not ambiguous here.)

With $P = gH/2$ the depth-averaged hydrostatic pressure, one retrieves the inviscid shallow-water model of Saint-Venant [17] when $\Sigma_{ij} = 0$, which coincides with Euler isentropic 2D flow model of perfect gases with $\gamma = 2$. Euler 2D model is (symmetric) hyperbolic and solutions to Cauchy problems allow one to numerically predict small-time evolutions of some compressible gases [14]. The shallow-water model of Saint-Venant is widely used e.g. in environmental hydraulics for nonlinear *irrotational* water waves in flat open channels with rugosity $k \geq 0$ [43], at least to predict the dynamics of *long surface waves*.

Moreover, the system (1–2) can also sustain shear motions. Formally, it approximates the depth-averaged free-surface Navier-Stokes equations for a viscous fluid with (small) viscosity $\nu \geq 0$ provided $\Sigma_{zz} = -(\Sigma_{xx} + \Sigma_{yy})$ and

$$\Sigma_{xx} = 2\nu\partial_x U \quad \Sigma_{yy} = 2\nu\partial_y V \quad \Sigma_{xy} = \nu(\partial_x V + \partial_y U) = \Sigma_{yx} \quad (3)$$

see [22, 30, 11] and references therein. An additional conservation law is satisfied:

$$\partial_t(HE) + \operatorname{div}(HE\mathbf{U} + H(P + \Sigma_{zz})\mathbf{U} - H\Sigma_h \cdot \mathbf{U}) = -kH|\mathbf{U}|^2 - HD, \quad (4)$$

with viscous dissipation $D = 2\nu(|D(\mathbf{U})|^2 + 2|\operatorname{div} \mathbf{u}|^2) \geq 0$ in shear, for

$$E = \frac{1}{2}(|\mathbf{U}|^2 + gH) \quad (5)$$

the so-called *mechanical energy*, convex in (H^{-1}, \mathbf{U}) . This is a formulation of the thermodynamics first principle when $k = 0 = \nu$ which implies, by Godunov-Mock theorem see e.g. [23], that the homogeneous system of conservation laws is (symmetric) *hyperbolic*. It also motivates the computation of small-time evolutions as L^2 solutions to Cauchy problems, see e.g. [40]. In particular, *entropy solutions* to Cauchy problems exist that satisfy the inequality (4)

$$\partial_t(HE) + \operatorname{div}(HE\mathbf{U} + H(P + \Sigma_{zz})\mathbf{U} - H\Sigma_h \cdot \mathbf{U}) \leq -kH|\mathbf{U}|^2 - HD \quad (6)$$

as a formulation of the thermodynamics second principle. Moreover, the 1D (translation-invariant) bounded measurable entropy solutions are unique since the system is also strictly hyperbolic when $H > 0$.

As soon as $\nu > 0$ however (e.g. to account for shear motions – 2D horizontal ones –), variations in the strain $D(\mathbf{U}) = (\nabla \mathbf{U} + \nabla \mathbf{U}^T)/2$ have an *infinite* propagation speed, and energy is dissipated everywhere in the strained fluid microstructure. This is not realistic for a number of flows, which may be better modelled as viscoelastic fluid continua of Maxwell type (i.e. fluids endowed with an energy storage capacity of elastic modulus G per unit mass and with a relaxation time λ that define a viscosity $\nu = G\lambda$ together).

2.2 Generalized Saint-Venant models for Maxwell fluids

In addition to a viscosity ν , viscoelastic fluids of Maxwell type are characterized by a time scale λ for the relaxation of the stress to a viscous state proportional to strain (it defines a Weissenberg number when compared with a time scale of the flow like $|\nabla \mathbf{U}|^{-1}$). Moreover, an evolution equation is also needed for Σ_{zz} and the horizontal stress *tensor*

$$\Sigma_h = \Sigma_{xx}\mathbf{e}_x \otimes \mathbf{e}_x + \Sigma_{yy}\mathbf{e}_y \otimes \mathbf{e}_y + \Sigma_{xy}\mathbf{e}_x \otimes \mathbf{e}_y + \Sigma_{yx}\mathbf{e}_y \otimes \mathbf{e}_x$$

to define a generalized Saint-Venant model for viscoelastic Maxwell fluids with $P = gH/2$. Various rate-type differential equations exist for the components of the tensor field Σ_h that are compatible with Galilean invariance.

Following the same depth-averaged analysis as in [22, 30] for viscous fluids, one can derive equations of the form $\lambda \overset{\Delta}{\Sigma} + \Sigma = 2\nu D(u, v, w)$ for the depth-averaged extra-stress variable $\Sigma = \Sigma_h + \Sigma_{zz}\mathbf{e}_z \otimes \mathbf{e}_z$ in a 3D Maxwell-fluid

model, using some admissible time-rate $\overset{\Delta}{\Sigma}$ (like the upper-convective derivative of Oldroyd-B model) and a steady equilibrium $\Sigma \approx 2\nu D(u, v, w)$ (typically compatible with (3)). Depending on scaling assumptions, various equations arise in [11], like (see [11, section 6.1.3.])

$$D_t \Sigma_h - L_h \Sigma_h - \Sigma_h L_h^T + \zeta (D_h \Sigma_h + \Sigma_h D_h^T) = (2\nu D_h - \Sigma_h)/\lambda \quad (7)$$

where $D_t := \partial_t + U\partial_x + V\partial_y \equiv \partial_t + \mathbf{U} \cdot \nabla$, $L_h := \nabla \mathbf{U}$, $D_h := (\mathbf{L}_h + \mathbf{L}_h^T)/2$, $\mathbf{W}_h := (\mathbf{L}_h - \mathbf{L}_h^T)/2$ for $\zeta = 0$, along with

$$D_t \Sigma_{zz} + 2(1 - \zeta) \operatorname{div} \mathbf{U} \Sigma_{zz} = (-2\nu \operatorname{div} \mathbf{U} - \Sigma_{zz})/\lambda. \quad (8)$$

Equivalently, with $\Sigma_{xy} = \Sigma_{yx}$, (7–8) reads

$$\begin{cases} D_t \Sigma_{xx} - (2(1 - \zeta) \Sigma_{xx} \partial_x U + \Sigma_{xy} ((2 - \zeta) \partial_y U - \zeta \partial_x V)) = (2\nu \partial_x U - \Sigma_{xx})/\lambda \\ D_t \Sigma_{yy} - (2(1 - \zeta) \Sigma_{yy} \partial_y V + \Sigma_{xy} (-\zeta \partial_y U + (2 - \zeta) \partial_x V)) = (2\nu \partial_y V - \Sigma_{yy})/\lambda \\ D_t \Sigma_{xy} - \left((1 - \zeta/2) (\Sigma_{xx} \partial_x V + \Sigma_{yy} \partial_y U) + (-\zeta/2) (\Sigma_{yy} \partial_x V + \Sigma_{xx} \partial_y U) \right. \\ \quad \left. + (1 - \zeta) \Sigma_{xy} (\partial_x U + \partial_y V) \right) = (\nu (\partial_x V + \partial_y U) - \Sigma_{xy})/\lambda \\ D_t \Sigma_{zz} + 2(1 - \zeta) \Sigma_{zz} (\partial_x U + \partial_y V) = (-2\nu (\partial_x U + \partial_y V) - \Sigma_{zz})/\lambda \end{cases}$$

which is Johnson-Segalman's 3D model¹ [27] with slip parameter $\zeta \in [0, 2]$ for some particular *incompressible* velocity fields (those without vertical shear).

The quasilinear system (1–2–7–8) for H , \mathbf{U} and $\mathbf{C} := \lambda \Sigma / \nu + \mathbf{I}$ is rotation-invariant. Then, it is easily computed that:

Proposition 2.1. *Only the slip-parameter value $\zeta = 0$ (i.e. the Upper-Convected case) ensures hyperbolicity of (1–2–7–8) under the strain-free constraints: $H > 0$, $C_{zz} > 0$ and \mathbf{C}_h be a symmetric positive definite tensor (thus also \mathbf{C}).*

The proof follows after computing the eigenvalues of the jacobian in a 1D projection of the system (1–2–7–8) like

$$\begin{cases} \partial_t h + \partial_x(hu) = 0 \\ \partial_t u + u\partial_x u + g\partial_x h - G((c_{xx} - c_{zz})/h\partial_x h + \partial_x(c_{xx} - c_{zz})) = 0 \\ \partial_t v + u\partial_x v - G(c_{xy}/h\partial_x h + \partial_x c_{xy}) = 0 \\ \partial_t c_{xx} + u\partial_x c_{xx} - (2(1 - \zeta)c_{xx}\partial_x u - \zeta\partial_x v) = 0 \\ \partial_t c_{yy} + u\partial_x c_{yy} - c_{xy}(2 - \zeta)\partial_x v = 0 \\ \partial_t c_{xy} + u\partial_x c_{xy} - ((1 - \zeta/2)c_{xx} - \zeta/2)c_{yy}\partial_x v - (1 - \zeta)c_{xy}\partial_x u = 0 \\ \partial_t c_{zz} + u\partial_x c_{zz} + 2(1 - \zeta)c_{zz}\partial_x u = 0 \end{cases} \quad (9)$$

similarly to the proof in [18] for a similar system written in stress variables Σ when $\zeta = 0$ (though without vertical stress and strain components, which allow

¹Recall that Johnson-Segalman's model uses the family of Gordon-Schowalter *objective* derivatives ($\zeta = 0$ is the upper-convected derivative, $\zeta = 1$ is Jauman derivative, $\zeta = 2$ is the lower-convected derivative) to cover a number of standard multidimensional generalizations of the Maxwell-fluid model: $\zeta = 0$ in Oldroyd-B model, $\zeta = 1$ in the co-rotational model and $\zeta = 2$ in Oldroyd-A model (with an additional purely-viscous stress characterized by a retardation-time).

here mass preservation). Denoting $\Delta = 2gh + G(2(3 - 2\zeta)c_{zz} + \zeta c_{yy} - 3\zeta c_{xx})$, four eigenvalues read

$$u \pm \frac{1}{2} \sqrt{\Delta + G((4 - 2\zeta)c_{xx} - 2\zeta c_{yy}) \pm \sqrt{\Delta^2 + G^2(4\zeta c_{xy})^2}}$$

and are real if, and only if, the following strain-parametrized inequality holds:

$$G^2(4\zeta c_{xy})^2 \leq 2G\Delta((4 - 2\zeta)c_{xx} - 2\zeta c_{yy}) + G^2((4 - 2\zeta)c_{xx} - 2\zeta c_{yy})^2$$

where, however, the strain values $c_{xx}, c_{yy}, c_{xy}, c_{zz}$ vanish when $\zeta = 0$. We therefore consider only (1-2-7-8) when $\zeta = 0$, where hyperbolicity is ensured with eigenvalues $u \pm \sqrt{gh + 3Gc_{zz} + Gc_{xx}}$, $u \pm \sqrt{Gc_{xx}}$ and u (with multiplicity 3) under the physically-natural constraints $h \geq 0, c_{zz} \geq 0, c_{xx} \geq 0$.

Indeed, at each point of the flow, \mathbf{C} can be interpreted as the expectation of $\mathbf{R}\mathbf{R}^T$ i.e. a *covariance* matrix for a stochastic material vector field \mathbf{R} that elastically deforms following the overdamped Langevin equation

$$d\mathbf{R} = \left(-(\mathbf{u} \cdot \nabla)\mathbf{R} + (\mathbf{L} - \zeta\mathbf{D})\mathbf{R} - \frac{1}{\lambda}\mathbf{R} \right) dt + \frac{1}{2\sqrt{\lambda}}d\mathbf{B}_t$$

under a Brownian field (\mathbf{B}_t) [34]. Alternatively, the stress $\Sigma = G(\mathbf{C} - \mathbf{I})$ is also reminiscent of a linear elastic (Hookean) material with elastic modulus $G = \nu/\lambda$, where the time-rate of \mathbf{C} would be that of a *left* Cauchy-Green deformation tensor $\mathbf{F}\mathbf{F}^T$ associated with a deformation gradient \mathbf{F} of time-rate $D_t\mathbf{F} - \nabla\mathbf{u}\mathbf{F}$. This is easily seen on rewriting Saint-Venant-Upper-Convected-Maxwell (SVUCM) model with constitutive equations:

$$D_t\mathbf{C}_h - \mathbf{L}_h\mathbf{C}_h - \mathbf{C}_h\mathbf{L}_h^T = (\mathbf{I} - \mathbf{C}_h)/\lambda, \quad (10)$$

$$D_t C_{zz} + 2C_{zz} \operatorname{div} \mathbf{U} = (1 - C_{zz})/\lambda. \quad (11)$$

As expected, the SVUCM model defined by the hyperbolic quasilinear system (1-2-10-11) on the domain $H, C_{zz}, \mathbf{C}_h = \mathbf{C}_h^T > 0$ preserves mass. Moreover, it formally satisfies the additional conservation law (4) with dissipation $D := G(\operatorname{tr} \mathbf{C} + \operatorname{tr} \mathbf{C}^{-1} - 2 \operatorname{tr} \mathbf{I})/(2\lambda) > 0$ for the Helmholtz free-energy

$$E = (|\mathbf{U}|^2 + gH + G \operatorname{tr}(\mathbf{C} - \ln \mathbf{C} - \mathbf{I})) / 2, \quad (12)$$

which suggests the following second thermodynamics principle formulation

$$\begin{aligned} & \partial_t(HE) + \partial_x(HEU + H(P + \Sigma_{zz} - \Sigma_{xx})U - H\Sigma_{xy}V) \\ & + \partial_y(HEV - H\Sigma_{yx}U + H(P + \Sigma_{zz} - \Sigma_{yy})V) \leq -kH|\mathbf{U}|^2 - HD \end{aligned} \quad (13)$$

on the admissibility domain $H, C_{zz}, \operatorname{tr} \mathbf{C}_h, \det \mathbf{C}_h > 0$ (where we use $\operatorname{tr} \ln \mathbf{C}_h = \ln \det \mathbf{C}_h$). Note that the free energy reads $E = (U^2 + V^2)/2 + E_H + E_\Sigma$ with Saint-Venant's potential energy $E_H = gH/2$ plus a Hookean contribution

$$E_\Sigma(\mathbf{C}) \equiv E_{\Sigma_h} + E_{\Sigma_{zz}} = G(\operatorname{tr}(\mathcal{E}(\mathbf{C}_h)) + \mathcal{E}(C_{zz})) / 2$$

where the function $\mathcal{E}(x) := x - \ln x - 1$ is convex in $x > 0$, but the system (1-2-7-8) is not in purely conservative form so one cannot straightforwardly apply Godunov-Mock theorem to show (symmetric) hyperbolicity of the system. However, E is useful to hyperbolicity: formally, the physically-admissible

solutions to Cauchy problems that satisfy (13) (and have admissible initial value in the hyperbolicity domain) preserve $C_{zz}, \text{tr } \mathbf{C}_h, \det \mathbf{C}_h > 0$.

However, note that there is a discrepancy in between the strain measure $(\mathbf{I} - \mathbf{F}^{-T} \mathbf{F}^{-1})/2$ naturally associated with the *left* Cauchy-Green (specific) deformation tensor $\mathbf{F} \mathbf{F}^T$ (usually termed Euler-Almansi) and the definition of the elastic stress $\mathbf{\Sigma}$. That is why, we also propose another model where (1–2) is coupled through $\mathbf{\Sigma}_h = G(\mathbf{I} - \mathbf{C}_h)$, $\Sigma_{zz} = G(1 - C_{zz})$ to

$$D_t \mathbf{C}_h + \mathbf{L}_h \mathbf{C}_h + \mathbf{C}_h \mathbf{L}_h^T = (\mathbf{I} - \mathbf{C}_h)/\lambda, \quad (14)$$

$$D_t C_{zz} - 2C_{zz} \text{div } \mathbf{U} = (1 - C_{zz})/\lambda. \quad (15)$$

Indeed, using for the time-rate of \mathbf{C} that of the *inverse* left Cauchy-Green deformation tensor (sometimes termed Finger deformation tensor) seems more consistent with the definition of (linear) elastic stresses $\mathbf{\Sigma}$ as a function of a (Euler-Almansi) strain measure. Note that the time-rate tensor in (14–15) is Galilean-invariant and induces an objective Maxwell-fluid law. It has been used previously in another context where 2D *weakly-sheared* flows also appear [45, 44, 21] and this is why we call this a Saint-Venant-Teshukov-Maxwell (SVTM) model. The SVTM model is rotation-invariant. Then, a 1D projection like

$$\left\{ \begin{array}{l} \partial_t h + \partial_x(hu) = 0 \\ \partial_t u + u\partial_x u + g\partial_x h + G((c_{xx} - c_{zz})/h\partial_x h + \partial_x(c_{xx} - c_{zz})) = 0 \\ \partial_t v + u\partial_x v + G(c_{xy}/h\partial_x h + \partial_x c_{xy}) = 0 \\ \partial_t c_{xx} + u\partial_x c_{xx} + 2c_{xx}\partial_x u = 0 \\ \partial_t c_{yy} + u\partial_x c_{yy} + 2c_{xy}\partial_x v = 0 \\ \partial_t c_{xy} + u\partial_x c_{xy} + c_{xy}\partial_x u + c_{xx}\partial_x v = 0 \\ \partial_t c_{zz} + u\partial_x c_{zz} - 2c_{zz}\partial_x u = 0 \end{array} \right. \quad (16)$$

again suffices (using lower-case notations for 1D systems) to see that the system is hyperbolic (strictly) on the same admissibility domain as SVUCM:

$$\{h, c_{xx}, c_{yy}, c_{zz} > 0; \quad (u, v) \in \mathbb{R}^2; \quad c_{xx}c_{yy} > c_{xy}^2\}.$$

In system (16) for $Q = (h, u, v, c_{xx}, c_{xy}, c_{yy}, c_{zz})$, the jacobian has eigenvalues:

$$\lambda_0 = u \text{ (with multiplicity 3)}, \lambda_{1\pm} = u \pm \sqrt{Gc_{xx}}, \lambda_{2\pm} = u \pm \sqrt{gh + G(3c_{xx} + c_{zz})}.$$

The SVTM model satisfies the same mass and energy conservation laws as SVUCM, but the laws (and the interpretations) of the dependent variable \mathbf{C} are not the same, as we shall observe in numerical illustrations of Section 4.

Finally, to sum up, we can now propose two hyperbolic quasilinear systems with zero retardation time as models for viscoelastic incompressible shallow free-surface 3D flows under gravity, which generalizes Saint-Venant's approach from a Newtonian fluid to Maxwell-type fluids.

The first 2D model is one particular case of the depth-averaged model formally derived in [11]. It bears similarities with the hyperbolic model of [38, 18, 25, 24] for compressible viscoelastic flows. In comparison, note that our model applies to incompressible flows and *conserves mass*, although it remains

mostly 2D. The improvement is obtained thanks to the introduction of a free-surface and assuming a stratified flow (i.e. vertical acceleration is neglected and a vertical velocity can be reconstructed from mass conservation), with a total (specific) pressure $P + \Sigma_{zz}$ decomposing into a hydrostatic component P plus an elastic component Σ_{zz} hence it holds

$$D_t(P + \Sigma_{zz}) + \left(P + \frac{2}{G}\Sigma_{zz} + 2 \right) \operatorname{div} \mathbf{U} = 0$$

to be compared with $D_t(P + \Sigma_{zz}) + \gamma(P + \Sigma_{zz}) \operatorname{div} \mathbf{U} = 0$ in [38, 18, 25, 24].

The second 2D model is an alternative to the first one which also conserves mass and is compatible with a formulation of thermodynamics principles. It has a more clear stress-strain relationship than the first model. It has been used previously to model eddies-microstructures in (weakly-sheared) turbulent flows.

Note that the two models contain similar closed subsystems that fully describe the 1D motions, for $q_1 = (h, u, c_{zz}, c_{xx})$ in solutions invariant e.g. by translation along \mathbf{e}_y . In SVUCM case, this is the 1D model that we proposed in [10], and whose Riemann initial-value problem has been completely solved in [12]. In SVTM case, the 1D system reads similarly except that c_{xx} and c_{zz} exchange their roles. This is natural insofar as their interpretation as strain components has been inverted ! One should keep in mind the inverted interpretations of the variable \mathbf{C} as deformations (in SVUCM) or as inverse deformations (in SVTM), in particular to read numerical results in Section 4.

3 Computational schemes for Cauchy problems

3.1 A framework for Riemann-based Finite-Volume schemes

With a view to numerically simulating time evolutions of flows governed by our models SVUCM and SVTM, we consider now computable approximations of solutions to Cauchy problems for the hyperbolic quasilinear systems.

We study carefully the SVTM case (1–2–14–15) with $P = gH/2$ and $\Sigma_h = G(\mathbf{I} - \mathbf{C}_h)$, $\Sigma_{zz} = G(1 - C_{zz})$

$$\begin{aligned} \partial_t H + \operatorname{div}(H\mathbf{U}) &= 0 \\ \partial_t(H\mathbf{U}) + \operatorname{div}(H\mathbf{U} \otimes \mathbf{U} + gH^2/2 - GHC_{zz} + GHC_h) &= -kH\mathbf{U} \\ \partial_t \mathbf{C}_h + \mathbf{U} \cdot \nabla \mathbf{C}_h + \mathbf{L}_h \mathbf{C}_h + \mathbf{C}_h \mathbf{L}_h^T &= (\mathbf{I} - \mathbf{C}_h)/\lambda \\ \partial_t C_{zz} + \mathbf{U} \cdot \nabla C_{zz} - 2C_{zz} \operatorname{div} \mathbf{U} &= (1 - C_{zz})/\lambda \end{aligned}$$

first, then a similar numerical scheme will follow for SVUCM (1–2–10–11)

$$\begin{aligned} \partial_t H + \operatorname{div}(H\mathbf{U}) &= 0 \\ \partial_t(H\mathbf{U}) + \operatorname{div}(H\mathbf{U} \otimes \mathbf{U} + gH^2/2 + GHC_{zz} - GHC_h) &= -kH\mathbf{U} \\ \partial_t \mathbf{C}_h + \mathbf{U} \cdot \nabla \mathbf{C}_h - \mathbf{L}_h \mathbf{C}_h - \mathbf{C}_h \mathbf{L}_h^T &= (\mathbf{I} - \mathbf{C}_h)/\lambda \\ \partial_t C_{zz} + \mathbf{U} \cdot \nabla C_{zz} + 2C_{zz} \operatorname{div} \mathbf{U} &= (1 - C_{zz})/\lambda \end{aligned}$$

with $\Sigma_h = G(\mathbf{C}_h - \mathbf{I})$, $\Sigma_{zz} = G(C_{zz} - 1)$ as explained in Section 3.4, on noting that both models have the same admissibility domain for the variable \mathbf{C} , the

same equilibrium, and that smooth solutions satisfy the same additional conservation law (4) in both cases (though we recall that the physical interpretations of the variable \mathbf{C} are inversed one another in between the two models).

We are not aware of a general theory that ensures the existence of a *unique* solution to Cauchy initial-value problems for *multidimensional nonlinear* hyperbolic systems like SVTM (or SVUCM) model. For instance, the 2D Saint-Venant system of conservation laws (formally reached in the limit $G \rightarrow 0$), which is symmetric and strictly hyperbolic, may have multiple *entropy solutions* [15].

Yet, full-2D admissible solutions can be approximated *stably* with a *Riemann-based* Finite-Volume (FV) method, using a piecewise-constant discretization of the unknown fields $H, \mathbf{U}, \mathbf{C}$ on the cells V_i ($i \in \mathbb{N}$) of a mesh [29].

In Riemann-based FV methods, one only needs numerical fluxes built from 1D Riemann problems (formula (17) below). Riemann problems have simple (self-similar) solutions in 1D, and they can typically be shown *well-posed* (with *entropy solutions*) for strictly hyperbolic systems of genuinely-nonlinear conservation laws, either by the vanishing-viscosity method or (equivalently) by the front-tracking method [6].

Recall however that our models are not full sets of conservation laws here. Defining univoque solutions to Riemann problems for the 1D SVTM system (16) may then be an issue because of non-conservative products, see e.g. [5] for a discussion of the problem and solutions. One solution has been used in [10, 12] to univoquely define (approximate) 1D Riemann solutions for the closed 4×4 subsystem in (h, uc_{xx}, c_{zz}) , because the non-conservative variables correspond to linearly degenerate fields and the mathematical entropy HE remains convex on the Hugoniot loci. But that solution method does not straightforwardly apply anymore here insofar as a non-conservative variable is not linearly degenerate.

Pragmatically though (i.e. for numerical purposes), we only need univoque *numerical fluxes*. That is the reason why we are naturally led to using only *approximate* (simple) 1D Riemann solvers which use only simple solutions (with only a few degrees of freedom) that are explicitly constrained to satisfy only the few consistency conditions identified so far, see e.g. [9].

We will construct in Section 3.2 *univoque* physically-admissible simple (approximate) solutions to 1D Riemann problems (without source term), thanks to a *frame-invariant* Riemann solver ensuring a discrete version of our formulation of thermodynamics principles (for the homogeneous systems with $k = 0$).

Now, a framework exists such that a “good” simple Riemann solver ensures the consistency of Riemann-based FV approximations with solutions to the homogeneous system. Moreover we also have to handle a source term. So, before defining precisely solutions to 1D Riemann homogeneous problems, let us first recall that FV framework from [9] and how to deal with the source term.

Given a tessellation of \mathbb{R}^2 using polygonal cells V_i , $i \in \mathbb{N}$, we write $q_h = \sum_i q_i(t)1_{V_i}$ the FV discretization of a 7-dimensional state vector q for SVTM model. (See below why we do not choose $Q \equiv (h, u, v, c_{xx}, c_{yy}, c_{xy}, c_{zz})$ as discretization variable q for (16).) We would like to solve a Cauchy problem for $q_h(t)$, $t \geq 0$ given some admissible q_h^0 at $t = 0 \equiv t^0$.

3.1.1 Splitting the time integration of FV approximations

We use a splitting method to divide time-integration at time $t^n = \sum_{k=0}^{n-1} \tau^k$, $n = 1 \dots N$ ($\tau^k > 0$) into two sub-steps: first, the differential terms are integrated

forward in time; second, the source terms are integrated backward in time.

For time step $[t^n, t^{n+1})$, we start with $q_h^n \approx q(t^n)$ and first have to compute the solution $q_h^{n+1,-} = \sum_i q_i^{n+1,-} 1_{V_i}$ at $t^{n+1,-}$ of the Cauchy problem for the *homogeneous* SVTM model on $[t^n, t^{n+1})$ with a forward-Euler time scheme.

Denoting $\mathbf{n}_{i \rightarrow j}$ the unit normal at a face $\Gamma_{ij} \equiv \overline{V_i} \cap \overline{V_j}$ oriented from V_i to V_j , we compute $q_h^{n+1,-}$ with a FV approximation on each control volume V_i

$$q_i^{n+1,-} = q_i^n - \tau^n \sum_{\Gamma_{ij} \equiv \overline{V_i} \cap \overline{V_j} \neq \emptyset} \frac{|\Gamma_{ij}|}{|V_i|} \mathbf{F}_{i \rightarrow j}(q_i^n, q_j^n; \mathbf{n}_{i \rightarrow j}) \quad (17)$$

that is consistent with a time-integration of our *frame-invariant model without source term*. In particular, discrete conservation laws hold for H_i and $H_i \mathbf{U}_i$ with consistent numerical fluxes $\mathbf{F}_{i \rightarrow j}^{H, HU}(q_i, q_j; \mathbf{n}_{i \rightarrow j})$ for the H and HU components of q : the latter should equal the normal flux components $\mathbf{F}^{H, HU}(q) \cdot \mathbf{n}_{i \rightarrow j}$ when $q = q_i = q_j$, and satisfy $\mathbf{F}_{i \rightarrow j}^{H, HU}(q_i, q_j; \mathbf{n}_{i \rightarrow j}) + \mathbf{F}_{j \rightarrow i}^{H, HU}(q_j, q_i; \mathbf{n}_{j \rightarrow i}) = 0$. For the other components, they are a priori solutions to non-conservative equations and it is still not clear which consistency conditions should be satisfied for them at this stage. . . except i) the additional conservation law for HE , which we require here as the (Clausius-Duhem) *inequality* (6), and ii) the *frame-invariance*, which is preserved if we use a frame-invariant 1D Riemann solver.

We will define *only in the next Section 3.2* such a numerical flux of the form

$$\mathbf{F}_{i \rightarrow j}(q_i, q_j; \mathbf{n}_{i \rightarrow j}) = \mathbf{O}_{i,j} \tilde{\mathbf{F}}(\mathbf{O}_{i,j}^{-1} q_i, \mathbf{O}_{i,j}^{-1} q_j) \quad (18)$$

that preserves the frame invariance and uses a flux $\tilde{\mathbf{F}}$ consistent for 1D Riemann problems, where $\mathbf{O}_{i,j}^{-1} q$ denotes a vector state variable with components in the local basis $(\mathbf{n}_{i \rightarrow j}, \mathbf{n}_{i \rightarrow j}^\perp)$ computed from the FV vector state q defined in a fixed reference frame $(\mathbf{e}_x, \mathbf{e}_y)$ and $\mathbf{O}_{i,j}$ denotes the inverse operation.

Still, at this point, we can already recall standard *stability properties* that shall be transferred to the FV approximation if the numerical flux is well chosen.

If the 1D Riemann solver $\tilde{\mathbf{F}}$ satisfies some stability constraints, then one can ensure stability properties for the FV approximation $q_h^{n+1,-}$ of the homogeneous hyperbolic system like the preservation of admissible domains, or discrete second-principle formulations (under conditions, like CFL: see below).

3.1.2 Sub-step 1: requiring CFL and entropy-consistency conditions

Let us consider numerical fluxes in (17–18) of the form

$$\begin{aligned} \tilde{\mathbf{F}}_{i \rightarrow j}(\mathbf{O}_{i,j}^{-1} q_i, \mathbf{O}_{i,j}^{-1} q_j) \\ = \mathbf{O}_{i,j}^{-1} \mathbf{F}(q_i) \mathbf{n}_{i \rightarrow j} - \int_{-\infty}^0 (R(\xi, \mathbf{O}_{i,j}^{-1} q_i, \mathbf{O}_{i,j}^{-1} q_j) - \mathbf{O}_{i,j}^{-1} q_i) d\xi \end{aligned} \quad (19)$$

using a simple 1D Riemann solver R with finite maximal wavespeed $s(q_l, q_r) > 0$, which is consistent with conservation laws (when relevant: recall here only components H and HU in q would satisfy conservation laws, a priori). If the Riemann solver preserves some physically-meaningful domain like (invariant)

sets convex in the discretization variable q , so will (17–18–19) do on noting

$$q_i^{n+1,-} = q_i^n \left(1 - \tau^n \sum_j \frac{|\Gamma_{ij}| s(\mathbf{O}_{i,j}^{-1} q_i^n, \mathbf{O}_{i,j}^{-1} q_j^n)}{|V_i|} \right) + \sum_j \frac{|\Gamma_{ij}|}{|V_i|} \int_{-s(\mathbf{O}_{i,j}^{-1} q_i^n, \mathbf{O}_{i,j}^{-1} q_j^n) \tau^n}^0 \mathbf{O}_{i,j} R(x/\tau^n, \mathbf{O}_{i,j}^{-1} q_i^n, \mathbf{O}_{i,j}^{-1} q_j^n) dx \quad (20)$$

is a convex combination, under the CFL condition

$$\forall i \quad \tau^n \sum_j \frac{|\Gamma_{ij}| s(\mathbf{O}_{i,j}^{-1} q_i^n, \mathbf{O}_{i,j}^{-1} q_j^n)}{|V_i|} \leq 1. \quad (21)$$

Proposition 3.1. *Under CFL condition (21), the FV time-integration formula (17) with flux (18) based on the 1D Riemann solver (19) preserves state sets that are convex in the discretization variable q .*

Moreover, a more stringent CFL condition with $s_i^n := \max_j s(\mathbf{O}_{i,j}^{-1} q_i^n, \mathbf{O}_{i,j}^{-1} q_j^n)$

$$\Delta t^n s_i^n \leq \left(\sum_j \frac{|\Gamma_{ij}|}{|V_i|} \right)^{-1} \quad (22)$$

may allow one to use Jensen inequality with the convex combination

$$q_i^{n+1,-} = \sum_j \frac{|\Gamma_{ij}|}{|V_i|} \int_{-\left(\sum_j \frac{|\Gamma_{ij}|}{|V_i|}\right)^{-1}}^0 \mathbf{O}_{i,j} R(x/\tau^n, \mathbf{O}_{i,j}^{-1} q_i^n, \mathbf{O}_{i,j}^{-1} q_j^n) dx, \quad (23)$$

so as to ensure *not only the decay of functionals $S(q)$ convex in q* (already ensured by (20) when the Riemann solver preserves convex invariant sets) but also a consistent discrete version of a *second-principle formulation* like

$$\partial_t S(q) + \operatorname{div} \mathbf{G}(q) \leq 0 \quad (24)$$

whenever (24) holds for some “mathematical entropy” $S(q)$ that is a convex function of the *Galilean invariants* of the state q with “entropy-flux” $\mathbf{G}(q)$, *under additional entropy-consistency conditions* on the solver (see (27) below). The consistency of numerical approximations with second-principle inequalities is essential to possibly converge to physically admissible *entropy solutions* [16].

Now, recall the SVTM model (1–2–14–15) is complemented by (13) i.e.

$$\begin{aligned} \partial_t (HE) + \partial_x (HEU + H(P + C_{xx} - C_{zz})U + HC_{xy}V) \\ + \partial_y (HEV + HC_{yx}U + H(P + C_{yy} - C_{zz})V) \leq -kH|U|^2 - HD \end{aligned} \quad (25)$$

with $D = -G(4 - \operatorname{tr} \mathbf{C}_h - \operatorname{tr} \mathbf{C}_h^{-1} + 2 - C_{zz} - C_{zz}^{-1})/(2\lambda) \geq 0$ for $E = (U^2 + V^2)/2 + E_H + E_\Sigma$ where $E_H = gH/2$, $E_\Sigma(\mathbf{C}) = G(\operatorname{tr}(\mathcal{E}(\mathbf{C}_h)) + \mathcal{E}(C_{zz}))/2$, and $\mathcal{E}(x) := x - \ln x - 1$. Then, we consider $S = HE$ as a mathematical entropy for the SVTM system without source term $k = 0 = D$ (in the first sub-step of our time-splitting scheme). The inequality (25) shows that a second-principle formulation (24) holds with an entropy flux $\mathbf{G} = HEU + H(P + \Sigma_{zz})U - H\Sigma_h \cdot U$.

So first, with a view to using Jensen inequality with (23), we can already choose a FV discretization variable q with a convex admissible set such that $S \equiv HE$ is convex in q at this stage. We propose

$$q := \left(H, HU, HV, HC_{xx}, HC_{yy}, HC_{xy}/\sqrt{C_{xx}C_{yy}}, HC_{zz} \right) \quad (26)$$

which has a convex admissible domain $q_1, q_4, q_5, q_7 > 0, |q_6| < q_1$ and such that $S/H \equiv E$ is convex in $(H^{-1}, U, V, C_{xx}, C_{yy}, C_{xy}/\sqrt{C_{xx}C_{yy}}, C_{zz})$, recall [9, Lemma 1.4].

Note however that the Riemann problems at interfaces Γ_{ij} will be solved for another variable \tilde{q} , see Section 3.2. So, let us stress again that the operators $\mathbf{O}_{i,j}^{-1}$ are *nonlinear*² (functions of the vector representation q of the state in a fixed Cartesian reference frame $\mathbf{e}_x, \mathbf{e}_y$), as well as the inverse operators $\mathbf{O}_{i,j}$ (functions of the vector representation \tilde{q} of the state in a local Cartesian basis $\mathbf{n}_{i \rightarrow j}, \mathbf{n}_{i \rightarrow j}^\perp$).

Next, to complete the first sub-step of our time-splitting scheme (a homogeneous Riemann problem), we propose to build a 1D Riemann solver that satisfies the following *entropy-consistency condition*: there exists a *conservative* discrete entropy-flux $\tilde{G}(q_l, q_r) = -\tilde{G}(q_r, q_l)$, *consistent* in FV sense with (24)

$$\tilde{G}(\mathbf{O}_{i,j}^{-1}q, \mathbf{O}_{i,j}^{-1}q) = \mathbf{G}(\mathbf{O}_{i,j}^{-1}q) \cdot \mathbf{e}_x = \mathbf{G}(q) \cdot \mathbf{n}_{i \rightarrow j}$$

for all admissible states q , such that for any admissible states q_l, q_r there holds

$$\begin{aligned} \mathbf{G}(q_r) \cdot \mathbf{e}_x + \int_0^{+\infty} (S(R(\xi, q_l, q_r)) - S(q_r)) d\xi \\ \leq \tilde{G}(q_l, q_r) \leq \mathbf{G}(q_l) \cdot \mathbf{e}_x - \int_{-\infty}^0 (S(R(\xi, q_l, q_r)) - S(q_l)) d\xi. \end{aligned} \quad (27)$$

Indeed, using $\int_0^{+\infty} S(R(\xi, q_l, q_r)) d\xi = -\int_{-\infty}^0 S(R(\xi, q_r, q_l)) d\xi$ and (27) we obtain

$$\begin{aligned} \int_{-s_i^n \tau^n}^0 S(\mathbf{O}_{i,j} R(x/\tau^n, \mathbf{O}_{i,j}^{-1}q_i^n, \mathbf{O}_{i,j}^{-1}q_j^n)) dx = \int_{-s_i^n \tau^n}^0 S(R(x/\tau^n, \mathbf{O}_{i,j}^{-1}q_i^n, \mathbf{O}_{i,j}^{-1}q_j^n)) dx \\ \leq (\tau^n s_i^n) S(q_i^n) - \tau^n \left(\tilde{G}(\mathbf{O}_{i,j}^{-1}q_i^n, \mathbf{O}_{i,j}^{-1}q_j^n) - \mathbf{G}(q_i^n) \cdot \mathbf{n}_{i \rightarrow j} \right) \end{aligned} \quad (28)$$

²The operators would degenerate as linear functions of the vector state only if we used the same representation at each step of the algorithm. Then, the operations would simply consist in a – linear – change of frame with coefficients *quadratic* in the components of the rotation matrix

$$\mathbf{\Omega}_{ij} = \begin{pmatrix} \mathbf{n}_{i \rightarrow j} \cdot \mathbf{e}_x & \mathbf{n}_{i \rightarrow j}^\perp \cdot \mathbf{e}_x \\ \mathbf{n}_{i \rightarrow j} \cdot \mathbf{e}_y & \mathbf{n}_{i \rightarrow j}^\perp \cdot \mathbf{e}_y \end{pmatrix}$$

here, because \mathbf{C}_h are components of a (2-contravariant) 2-tensor variable.

and finally, with (23), a consistent discrete second-principle formulation:

$$\begin{aligned} S(q_i^{n+1,-}) - S(q_i^n) + \tau^n \sum_j \frac{|\Gamma_{ij}|}{|V_i|} \tilde{G}(\mathbf{O}_{i,j}^{-1} q_i^n, \mathbf{O}_{i,j}^{-1} q_j^n) \\ \leq \tau^n \sum_j \frac{|\Gamma_{ij}|}{|V_i|} \mathbf{G}(q_i^n) \cdot \mathbf{n}_{i \rightarrow j} \equiv 0. \end{aligned} \quad (29)$$

Proposition 3.2. *Under CFL condition (22), the FV time-integration formula (17) with flux (18) based on a 1D Riemann solver (19)*

- *preserves convex state sets in the FV discretization variable q and*
 - *satisfies the discrete version (29) of the second-principle formulation (25) (with $k = 0 = D$) provided*
1. *$S = HE$ is a convex function of q , and*
 2. *the entropy-consistency condition (27) is satisfied for some \tilde{G} .*

We propose in next Section 3.2 a solver R satisfying (27) for some \tilde{G} .

3.1.3 Sub-step 2: integrating source terms with Backward-Euler

To complete the time-integration of our SVTM model, we standardly propose a second sub-step using the backward-Euler time-scheme for the source terms

$$\mathbf{U}(q_i^{n+1}) - \mathbf{U}(q_i^{n+1,-}) = -\tau^n k \mathbf{U}(q_i^{n+1}) \quad (30)$$

$$\mathbf{C}_h(q_i^{n+1}) - \mathbf{C}_h(q_i^{n+1,-}) = \frac{\tau^n}{\lambda} (\mathbf{I} - \mathbf{C}_h(q_i^{n+1})) \quad (31)$$

$$C_{zz}(q_i^{n+1}) - C_{zz}(q_i^{n+1,-}) = \frac{\tau^n}{\lambda} (1 - C_{zz}(q_i^{n+1})) \quad (32)$$

with $H_i^{n+1} = H_i^{n+1,-}$ (mass is conserved), the time step τ^n being given by the CFL condition (22) of sub-step 1. An *admissible* state $\mathbf{U}(q_i^{n+1}), \mathbf{C}_h(q_i^{n+1}), C_{zz}(q_i^{n+1})$ can be computed *explicitly* here as a convex combination of admissible states, insofar as the source terms RHS in (30), (31), (32) are all *linear* in $\mathbf{U}, \mathbf{C}_h, C_{zz}$, of relaxation type. (We only need *explicit* nonlinear mappings for the variable change $(H, \mathbf{U}, \mathbf{C}_h, C_{zz}) \leftrightarrow q$ *cellwise*.)

A discrete version of (25) is satisfied (with $D \neq 0$ like in (25))

$$\begin{aligned} S(q_i^{n+1}) - S(q_i^n) + \tau^n \sum_j \frac{|\Gamma_{ij}|}{|V_i|} \tilde{G}(\mathbf{O}_{i,j}^{-1} q_i^n, \mathbf{O}_{i,j}^{-1} q_j^n) \\ \leq -\tau^n k |\mathbf{U}_i^{n+1}|^2 - \tau^n D(q_i^{n+1}) \end{aligned} \quad (33)$$

which can be shown from (29) and the convexity of $S = HE$ hence, for instance,

$$\begin{aligned} E_\Sigma(\mathbf{C}_h(q_i^{n+1})) - E_\Sigma(\mathbf{C}_h(q_i^{n+1,-})) \\ \leq (\mathbf{I} - \mathbf{C}_h(q_i^{n+1})^{-1}) : (\mathbf{C}_h(q_i^{n+1}) - \mathbf{C}_h(q_i^{n+1,-})) \end{aligned} \quad (34)$$

where $(\mathbf{I} - \mathbf{C}_h(q_i^{n+1})^{-1}) : (\mathbf{I} - \mathbf{C}_h(q_i^{n+1})) \leq 0$ is one term of the dissipation $D(q_i^{n+1})$ (for a detailed proof of (34), see e.g. [3, (2.7e) in Lemma 2.1]).

3.2 A 5-wave relaxation solver

To follow the general framework presented in Section 3.1 for Riemann-based FV discretizations, let us start here the construction of an entropy-consistent *simple* Riemann solver $R(\zeta, \mathbf{O}_{i,j}^{-1}q_i, \mathbf{O}_{i,j}^{-1}q_j)$. Precisely, we explicitly define approximate solutions to 1D Riemann problems for the quasilinear (non-conservative) SVTM 1D system (16) that are piecewise-constant functions of the self-similarity variable ζ with finitely-many values. We next show that the entropy-consistency condition (27) can be satisfied, so the Riemann solver conforms with the general framework presented in Section 3.1. We recall that the SVUCM system will be treated afterwards in Section 3.4, with an approach similar to that for SVTM.

To start with, let us consider the system (16) for the variable

$$\tilde{q} := (h, hu, h^{-2}c_{xx}, h^2c_{zz}, h(c_{yy} - c_{xy}^2/c_{xx}), hc_{xy}/\sqrt{c_{xx}}, hv)$$

with left/right initial values $\mathbf{O}_{i,j}^{-1}q_i, \mathbf{O}_{i,j}^{-1}q_j$ computed in the local frame by

$$\begin{aligned} c_{xx} &= \mathbf{C}_h(q) \mathbf{n}_{i \rightarrow j} \cdot \mathbf{n}_{i \rightarrow j} \\ c_{xy} &= \mathbf{C}_h(q) \mathbf{n}_{i \rightarrow j}^\perp \cdot \mathbf{n}_{i \rightarrow j} = \mathbf{C}_h \mathbf{n}_{i \rightarrow j}^\perp \cdot \mathbf{n}_{i \rightarrow j} \\ c_{xy} &= \mathbf{C}_h(q) \mathbf{n}_{i \rightarrow j}^\perp \cdot \mathbf{n}_{i \rightarrow j}^\perp \end{aligned}$$

as *nonlinear* functions of the left/right values q_i, q_j .

For consistency, we require that Riemann solutions preserve $h, c_{xx}, c_{zz}, c_{yy} - c_{xy}^2/c_{xx} > 0$ i.e. admissibility, and mimic the second-principle formulation

$$\partial_t (h(E_\parallel + E_\perp)) + \partial_x (hu(E_\parallel + hE_\perp + uP_\parallel + vP_\perp)) \leq 0 \quad (35)$$

for the free-energy $h(E_\parallel + E_\perp)$ as mathematical entropy, with two terms

$$\begin{aligned} E_\parallel &= \frac{u^2}{2} + e_\parallel ; \quad e_\parallel = \frac{gh}{2} + \frac{G(c_{xx} + c_{zz})}{2} - \frac{G \ln(c_{xx}c_{zz})}{2} \\ E_\perp &= \frac{v^2}{2} + e_\perp ; \quad e_\perp = \frac{Gc_{xy}^2/c_{xx}}{2} + \frac{G(c_{yy} - c_{xy}^2/c_{xx})}{2} - \frac{G \ln(c_{yy} - c_{xy}^2/c_{xx})}{2} \end{aligned}$$

that satisfy independent conservation laws with two pressure terms

$$\partial_t (hE_\parallel) + \partial_x (hu_\parallel + uP_\parallel) = 0 \quad \partial_t (hE_\perp) + \partial_x (hvE_\perp + vP_\perp) = 0$$

$$P_\parallel = -\partial_{h^{-1}}|_{hc_{xx}^{-1/2}, hc_{zz}^{1/2}} e_\parallel = \frac{gh^2}{2} + Gh(c_{xx} - c_{zz}) \quad P_\perp = Ghc_{xy}$$

in smooth evolutions (without discontinuities) so as to define a consistent numerical entropy-flux \tilde{G} (our condition (27) for admissible discretizations). One issue is *first* give a meaning to the non-conservative nonlinear terms. Here, we straightforwardly devise a *simple* Riemann solver that univoquely approximates admissible 1D solutions. Rewriting the 1D SVTM model in \tilde{q} :

$$\left\{ \begin{aligned} \partial_t h + \partial_x (hu) &= 0 \\ \partial_t (hu) + \partial_x (hu^2) + \partial_x (gh^2/2) + \partial_x (Gh(c_{xx} - c_{zz})) &= 0 \\ \partial_t (h^{-2}c_{xx}) + u\partial_x (h^{-2}c_{xx}) &= 0 \\ \partial_t (h^2c_{zz}) + u\partial_x (h^2c_{zz}) &= 0 \\ \partial_t (c_{yy} - c_{xy}^2/c_{xx}) + u\partial_x (c_{yy} - c_{xy}^2/c_{xx}) &= 0 \\ \partial_t (hv) + \partial_x (huv) + \partial_x (Ghc_{xy}) &= 0 \\ \partial_t (h^{-1}c_{xy}) + u\partial_x (h^{-1}c_{xy}) + (h^{-2}c_{xx})h\partial_x v &= 0 \end{aligned} \right. \quad (36)$$

with a view to constructing a Riemann solver, our variable choice \tilde{q} for the 1D Riemann problems obviously justifies: there is actually *only one* non-conservative product (for the evolution of $c_{xy}h^{-1}$).

We next consider a *5-wave simple solver* for the system (36) in Euler coordinates (i.e. which uses a Eulerian flow description), after the standard transformation of a simple solver for (36) rewritten in Lagrange coordinates [20] i.e.

$$\left\{ \begin{array}{l} \partial_t h^{-1} - \partial_x u = 0 \\ \partial_t u + \partial_x (gh^2/2 + Gh(c_{xx} - c_{zz})) = 0 \\ \partial_t (h^{-2}c_{xx}) = 0 \\ \partial_t (h^2c_{zz}) = 0 \\ \partial_t (c_{yy} - c_{xy}^2/c_{xx}) = 0 \\ \partial_t v + \partial_x (Ghc_{xy}) = 0 \\ \partial_t (c_{xy}/h) + c_{xx}\partial_x v = 0 \end{array} \right. \quad (37)$$

which suggests a 5-wave (Lagrangian) solver inspired by Suliciu's relaxation strategy of pressures (a "general" strategy for fluids described in [9]). The additional conservations laws for (37) write

$$\partial_t E_{\parallel} + \partial_x (uP_{\parallel}) = 0 = \partial_t E_{\perp} + \partial_x (vP_{\perp})$$

for smooth solutions. Then, on noting smooth $P_{\parallel} = \frac{gh^2}{2} + Gh(c_{xx} - c_{zz})$ satisfy

$$\partial_t P_{\parallel} + c_{\parallel}^2 \partial_x u = 0$$

with $c_{\parallel}^2 = h^2(gh + G(3c_{xx} + c_{zz}))$, smooth $P_{\perp} = Ghc_{xy}$ satisfy

$$\partial_t P_{\perp} + b\partial_x u + c_{\perp}^2 \partial_x v = 0$$

with $b = 2Gh^2c_{xy}$ and $c_{\perp}^2 = Gh^2c_{xx}$, and smooth c_{xy}/h satisfy

$$\partial_t (c_{xy}/h) + a^2 \partial_x v = 0$$

with $a^2 = c_{xx}$, we propose the following relaxed approximation of (37)

$$\left\{ \begin{array}{l} \partial_t h^{-1} - \partial_x u = 0 \\ \partial_t u + \partial_x \pi_{\parallel} = 0 \\ \partial_t \pi_{\parallel} + c_{\parallel}^2 \partial_x u = 0 \\ \partial_t (c_{xy}/h) + a^2 \partial_x v = 0 \\ \partial_t v + \partial_x \pi_{\perp} = 0 \\ \partial_t \pi_{\perp} + b\partial_x u + c_{\perp}^2 \partial_x v = 0 \\ \partial_t (h^{-2}c_{xx}) = 0 \\ \partial_t (h^2c_{zz}) = 0 \\ \partial_t (c_{yy} - c_{xy}^2/c_{xx}) = 0 \end{array} \right. \quad (38)$$

which is a hyperbolic system with all fields linearly degenerate and thus allows one to compute easily approximate Riemann solutions in Lagrange coordinates.

The general Riemann solution to (38) has 5 waves with speeds $-c_{\parallel} < -c_{\perp} < 0 < c_{\perp} < c_{\parallel}$ that can be ordered consistently with the definition of the relaxation parameters in smooth evolution cases. Note the following relations

$$\begin{cases} \partial_t(\pi_{\parallel} + c_{\parallel}u) + c_{\parallel}\partial_x(\pi_{\parallel} + c_{\parallel}u) = 0 \\ \partial_t(\pi_{\parallel} - c_{\parallel}u) - c_{\parallel}\partial_x(\pi_{\parallel} - c_{\parallel}u) = 0 \\ \partial_t(\pi_{\parallel}/c_{\parallel}^2 + h^{-1}) = 0 \\ \partial_t(h^{-2}c_{xx}) = 0 \\ \partial_t(h^2c_{zz}) = 0 \end{cases} \quad (39)$$

hold for the q_1 -subsystem, already treated in [10] with same relaxation approach. So, the Riemann solution has the following structure (in any variable q)

$$\begin{cases} q_l & x < -c_{\parallel}t \\ q_l^* & -c_{\parallel}t < x < -c_{\perp}t \\ q_l^{\sharp} & -c_{\perp}t < x < 0 \\ q_r^{\sharp} & 0 < x < c_{\perp}t \\ q_r^* & c_{\perp}t < x < c_{\parallel}t \\ q_r & x > c_{\parallel}t \end{cases} \quad (40)$$

and \tilde{q}_1 can be explicated through the following analytical expressions

$$\begin{aligned} u_l^* &= u_r^* = u_l^{\sharp} = u_r^{\sharp} = u^* \equiv \frac{c_{\parallel}u_l + \pi_{\parallel,l} + c_{\parallel}u_r - \pi_{\parallel,r}}{2c_{\parallel}} \\ \pi_{\parallel,l}^* &= \pi_{\parallel,r}^* = \pi_{\parallel,l}^{\sharp} = \pi_{\parallel,r}^{\sharp} = \pi^* \equiv \frac{\pi_{\parallel,l} + c_{\parallel}u_l + \pi_{\parallel,r} - c_{\parallel}u_r}{2} \\ \frac{1}{h_l^*} &= \frac{1}{h_l^{\sharp}} = \frac{1}{h_l} \left(1 + \frac{c_{\parallel}(u_r - u_l) + \pi_{\parallel,l} - \pi_{\parallel,r}}{2c_{\parallel}^2/h_l} \right) \\ \frac{1}{h_r^*} &= \frac{1}{h_r^{\sharp}} = \frac{1}{h_r} \left(1 + \frac{c_{\parallel}(u_r - u_l) + \pi_{\parallel,r} - \pi_{\parallel,l}}{2c_{\parallel}^2/h_r} \right) \\ (h^{-2}c_{xx})_l^* &= (h^{-2}c_{xx})_l^{\sharp} = h^{-2}c_{xx} & (h^{-2}c_{xx})_r^* &= (h^{-2}c_{xx})_r^{\sharp} = h^{-2}c_{xx} \\ (h^2c_{zz})_l^* &= (h^2c_{zz})_l^{\sharp} = h^2c_{zz} & (h^2c_{zz})_r^* &= (h^2c_{zz})_r^{\sharp} = h^2c_{zz} \end{aligned} \quad (41)$$

(i.e. u, π_{\parallel} are weak Riemann invariants for c_{-1}, c_0, c_1 waves, $\pi_{\parallel}/c_{\parallel}^2 + h^{-1}, h^{-2}c_{xx}, h^2c_{zz}$ are weak Riemann invariants for c_{-2}, c_{-1}, c_1, c_2 waves, $\pi_{\parallel} - c_{\parallel}u$ for c_2 and $\pi_{\parallel} + c_{\parallel}u$ for c_{-2}) on recalling [10]. Note also

$$\begin{aligned} \partial_t(\pi_{\perp} + c_{\parallel}v) + c_{\parallel}\partial_x(\pi_{\perp} + c_{\parallel}v) + \partial_x(bu + (c_{\perp}^2 - c_{\parallel}^2)v) &= 0 \\ \partial_t(\pi_{\perp} - c_{\parallel}v) - c_{\parallel}\partial_x(\pi_{\perp} - c_{\parallel}v) + \partial_x(bu + (c_{\perp}^2 - c_{\parallel}^2)v) &= 0 \end{aligned} \quad (42)$$

where $bu + (c_{\perp}^2 - c_{\parallel}^2)v$ is a weak Riemann invariant for c_{-2}, c_2 waves like $a^2\pi_{\perp}/c_{\parallel}^2 - c_{xy}/h$. Moreover, $\pi_{\perp} - c_{\parallel}v$ is a weak c_2 invariant and $\pi_{\perp} + c_{\parallel}v$ a weak c_{-2}

invariant. The following analytical expressions then also hold

$$\begin{aligned}
v_l^* &= v_l + \frac{b}{c_\perp^2 - c_\parallel^2} (u_l - u^*) = v_l + \frac{b}{c_\perp^2 - c_\parallel^2} \frac{c_\parallel u_l - \pi_{\parallel,l} - c_\parallel u_r + \pi_{\parallel,r}}{2c_\parallel} \\
v_r^* &= v_r + \frac{b}{c_\perp^2 - c_\parallel^2} (u_r - u^*) = v_r + \frac{b}{c_\perp^2 - c_\parallel^2} \frac{c_\parallel u_r + \pi_{\parallel,r} - c_\parallel u_l - \pi_{\parallel,l}}{2c_\parallel} \\
\pi_{\perp,l}^* &= c_\parallel (v_l - v_l^*) + \pi_{\perp,l} = \pi_{\perp,l} + \frac{bc_\parallel}{c_\perp^2 - c_\parallel^2} \frac{c_\parallel u_r - \pi_{\parallel,r} - c_\parallel u_l + \pi_{\parallel,l}}{2c_\parallel} \\
\pi_{\perp,r}^* &= c_\parallel (v_r^* - v_r) + \pi_{\perp,r} = \pi_{\perp,r} + \frac{bc_\parallel}{c_\perp^2 - c_\parallel^2} \frac{c_\parallel u_r + \pi_{\parallel,r} - c_\parallel u_l - \pi_{\parallel,l}}{2c_\parallel} \\
(c_{xy}/h)_l^* &= (c_{xy}/h)_l + \frac{a^2}{c_\parallel^2} (\pi_{\perp,l}^* - \pi_{\perp,l}) = (c_{xy}/h)_l + \frac{a^2 b/c_\parallel}{c_\perp^2 - c_\parallel^2} \frac{c_\parallel u_r - \pi_{\parallel,r} - c_\parallel u_l + \pi_{\parallel,l}}{2c_\parallel} \\
(c_{xy}/h)_r^* &= (c_{xy}/h)_r + \frac{a^2}{c_\parallel^2} (\pi_{\perp,r}^* - \pi_{\perp,r}) = (c_{xy}/h)_r + \frac{a^2 b/c_\parallel}{c_\perp^2 - c_\parallel^2} \frac{c_\parallel u_r + \pi_{\parallel,r} - c_\parallel u_l - \pi_{\parallel,l}}{2c_\parallel}
\end{aligned} \tag{43}$$

and, on noting

$$\begin{aligned}
\partial_t(\pi_\perp + c_\perp v) + c_\perp \partial_x(\pi_\perp + c_\perp v) + b \partial_x u &= 0 \\
\partial_t(\pi_\perp - c_\perp v) - c_\perp \partial_x(\pi_\perp - c_\perp v) + b \partial_x u &= 0 \\
\partial_t(a^2 \pi_\perp - c_\perp^2 c_{xy}/h) + a^2 b \partial_x u &= 0
\end{aligned} \tag{44}$$

where u is a weak invariant for c_{-1}, c_0, c_1 , we get

$$\begin{aligned}
v_l^\# &= v_r^\# = v^\# \equiv \frac{c_\perp v_l^* + \pi_{\perp,l}^* + c_\perp v_r^* - \pi_{\perp,r}^*}{2c_\parallel} \\
\pi_{\perp,l}^\# &= \pi_{\perp,r}^\# = \pi_\perp^\# = \frac{\pi_{\perp,l}^* + c_\perp v_l^* + \pi_{\perp,r}^* - c_\perp v_r^*}{2} \\
(c_{xy}/h)_r^\# &= (c_{xy}/h)_r^* + \frac{a^2}{c_\perp^2} (\pi_\perp^\# - \pi_{\perp,r}^*) = (c_{xy}/h)_r^* + \frac{a^2}{c_\perp^2} \frac{\pi_{\perp,l}^* + c_\perp v_l^* - \pi_{\perp,r}^* - c_\perp v_r^*}{2} \\
(c_{xy}/h)_l^\# &= (c_{xy}/h)_l^* + \frac{a^2}{c_\perp^2} (\pi_\perp^\# - \pi_{\perp,l}^*) = (c_{xy}/h)_l^* + \frac{a^2}{c_\perp^2} \frac{\pi_{\perp,r}^* - c_\perp v_r^* - \pi_{\perp,l}^* + c_\perp v_l^*}{2}
\end{aligned} \tag{45}$$

which completes the expression of the Riemann solution of (38) with, for $o = l/r$

$$(c_{yy} - c_{xy}^2/c_{xx})_o = (c_{yy} - c_{xy}^2/c_{xx})_o^* = (c_{yy} - c_{xy}^2/c_{xx})_o^\#.$$

Now, we can propose a “pseudo-relaxed” Riemann solver for SVTM system

$$\left\{ \begin{aligned}
&\partial_t h + \partial_x(hu) = 0 \\
&\partial_t(hu) + \partial_x(hu^2 + \pi_\parallel) = 0 \\
&\partial_t(h\pi_\parallel) + \partial_x(hu\pi_\parallel) + c_\parallel^2 \partial_x u = 0 \\
&\partial_t c_{xy} + \partial_x(uc_{xy}) + a^2 hv = 0 \\
&\partial_t(hv) + \partial_x(huv + \pi_\perp) = 0 \\
&\partial_t(h\pi_\perp) + \partial_x(hu\pi_\perp + bu) + c_\perp^2 \partial_x v = 0 \\
&\partial_t(h^{-1}c_{xx}) + \partial_x(h^{-1}c_{xx}u) = 0 \\
&\partial_t(h^3 c_{zz}) + \partial_t(h^3 c_{zz}u) = 0 \\
&\partial_t(h(c_{yy} - c_{xy}^2/c_{xx})) + \partial_x(h(c_{yy} - c_{xy}^2/c_{xx})u) = 0
\end{aligned} \right. \tag{46}$$

in *Euler coordinates*, recalling the transformation of a simple Riemann solver from Lagrange to Euler coordinates [20]. Note that it has the same intermediate

states as the solver in Lagrange coordinates, but different wave-speeds, namely:

$$\begin{aligned}\xi_{-2} &= u_l - c_{\parallel}/h_l \equiv u^* - c_{\parallel}/h_l^* \\ \xi_{-1} &= u_l^* - c_{\perp}/h_l^* \equiv u_l^{\sharp} - c_{\perp}/h_l^{\sharp} \\ \xi_0 &= u^* \equiv \xi_0 \\ \xi_{+1} &= u_r^* + c_{\perp}/h_r^* \equiv u_r^{\sharp} + c_{\perp}/h_r^{\sharp} \\ \xi_{+2} &= u_r + c_{\parallel}/h_r \equiv u^* + c_{\parallel}/h_r^*\end{aligned}$$

which are obviously compatible with the weak Riemann invariants of each wave.

It remains to be seen whether the Riemann solver is actually “entropy-consistent”, i.e. condition (27) is satisfied. To that aim, let us add two unknowns $\hat{e}_{\parallel}, \hat{e}_{\perp}$ to (46) such that

$$\partial_t (h(u^2/2 + \hat{e}_{\parallel})) + \partial_x (hu(u^2/2 + \hat{e}_{\parallel}^2) + \pi_{\parallel}u) = 0 \quad (47)$$

$$\partial_t (h(v^2/2 + \hat{e}_{\perp})) + \partial_x (hv(v^2/2 + \hat{e}_{\perp}^2) + \pi_{\perp}v) = 0 \quad (48)$$

hold. On recalling the structure (40) of solutions to Riemann problems, if we use $(\hat{e}_{\parallel})_o = e_{\parallel}(q_o)$ and $(\hat{e}_{\perp})_o = e_{\perp}(q_o)$ for $o = l/r$ as left/right initial conditions, then the following holds:

Proposition 3.3. *If the six following inequalities hold, for $o = l/r$,*

$$e_{\parallel}(q_o^*) \leq (\hat{e}_{\parallel})_o^* \quad (49)$$

$$e_{\perp}(q_o^*) \leq (\hat{e}_{\perp})_o^* \quad (50)$$

$$e_{\perp}(q_o^{\sharp}) \leq (\hat{e}_{\perp})_o^{\sharp} \quad (51)$$

then the entropy-consistency condition (27) is satisfied³ with flux $\tilde{G} = [hu(u^2/2 + \hat{e}_{\parallel}^2 + v^2/2 + \hat{e}_{\perp}^2) + \pi_{\parallel}u + \pi_{\perp}v]_{x/t=0}$ (a c_0 Riemann invariant).

3.3 Choosing entropy-consistent relaxation parameters

We now explain how to satisfy the entropy-consistency conditions of Prop. 3.3 for the relaxation parameters $c_{\parallel}^2, c_{\perp}^2, a^2$.

Condition (49) is classically satisfied provided the following condition

$$h^2 \partial_h |_{hc_{xx}^{-1/2}, hc_{zz}^{+1/2}} P_{\parallel} = h^2 (gh + Gh(3c_{xx} + c_{zz})) \leq c_{\parallel}^2 \quad (53)$$

is satisfied for all h in between h_o and h_o^* , $o = l/r$, see [9, 10]. The first step to show (53) is to compute $(\hat{e}_{\parallel})_o^* = (\hat{e}_{\parallel})_o^{\sharp}$ from the equation (47), which can be done from the system in Lagrange coordinates augmented by the equation

$$\partial_t (u^2/2 + \hat{e}_{\parallel}) + \partial_x (u\pi_{\parallel}) = 0$$

³Note that it is of course not strictly necessary that (49) and (50) hold independently from one another, in fact it is sufficient that

$$(e_{\parallel} + e_{\perp})(q_o^*) \leq (\hat{e}_{\parallel} + \hat{e}_{\perp})_o^* \quad (52)$$

holds but it is easier to check (49) and (50) separately.

on noting that the following equation (in Lagrange coordinates) holds

$$\partial_t(u^2/2 + \pi_{\parallel}^2/2c_{\parallel}^2) + \partial_x(u\pi_{\parallel}) = 0$$

so $(\hat{e}_{\parallel})_o^* = (\hat{e}_{\parallel})_o^{\sharp}$ can be obtained from the solution of

$$\partial_t(\hat{e}_{\parallel} - \pi_{\parallel}^2/2c_{\parallel}^2) = 0.$$

The second step subtracts $(P_{\parallel}(q_o^*) - \pi_{\parallel}^*)^2/(2c_{\parallel}^2) \geq 0$ in the RHS of (49) rewritten

$$\left(e_{\parallel} - \frac{P_{\parallel}^2}{2c_{\parallel}^2}\right)(q_o^*) \leq \left(e_{\parallel} - \frac{P_{\parallel}^2}{2c_{\parallel}^2}\right)(q_o) + \frac{(\pi_{\parallel}^*)^2 - P_{\parallel}(q_o^*)^2}{2c_{\parallel}^2} \quad (54)$$

and uses the Riemann invariant $h^{-1} + \pi_{\parallel}/c_{\parallel}^2$ to show that, in fact,

$$\left(e_{\parallel} - \frac{P_{\parallel}^2}{2c_{\parallel}^2}\right)(h_o^*) \leq \left(e_{\parallel} - \frac{P_{\parallel}^2}{2c_{\parallel}^2}\right)(h_o) - P_{\parallel}(h_o^*) \left(\frac{1}{h_o^*} - \frac{1}{h_o} + \frac{P_{\parallel}(h_o^*) - P_{\parallel}(h_o)}{c_{\parallel}^2}\right)$$

is enough, and therefore (53) after looking at variations in h_o^* .

Similarly, the Riemann invariants $\hat{e}_{\perp} - \pi_{\perp}^2/2c_{\parallel}^2$ and $\hat{e}_{\perp} - \pi_{\perp}^2/2c_{\perp}^2$ give $(\hat{e}_{\perp})_o^*$ and $(\hat{e}_{\perp})_o^{\sharp}$. Then, on noting (42), a sufficient condition for (50) to hold reads

$$\begin{aligned} \left(e_{\perp} - \frac{P_{\perp}^2}{2c_{\parallel}^2}\right)(q_o^*) &\leq \left(e_{\perp} - \frac{P_{\perp}^2}{2c_{\parallel}^2}\right)(q_o) \\ &\quad - P_{\perp}(q_o^*) \left(\frac{P_{\perp}(q_o^*) - P_{\perp}(q_o)}{c_{\parallel}^2} - \left(\frac{c_{xy}}{a^2 h}\right)_o^* + \left(\frac{c_{xy}}{a^2 h}\right)_o\right) \end{aligned} \quad (55)$$

which rewrites with $\tilde{G}_o := \left(\frac{G c_{xx}}{h^2 c_{\parallel}^2}\right)_o = \left(\frac{G c_{xx}}{h^2 c_{\parallel}^2}\right)_o^*$ and $\tilde{\alpha}_o := \left(\frac{c_{xx}}{h^2 a^2}\right)_o = \left(\frac{c_{xx}}{h^2 a^2}\right)_o^*$

$$\begin{aligned} (1 - \tilde{G}_o(h_o^*)^4) \left(\left(\frac{c_{xy}}{h}\right)_o^*\right)^2 &\leq (1 - \tilde{G}_o h_o^4) \left(\left(\frac{c_{xy}}{h}\right)_o\right)^2 \\ &\quad - 2(h_o^*)^2 \left(\frac{c_{xy}}{h}\right)_o^* \left(\tilde{G}_o(h_o^*)^2 - \tilde{\alpha}_o\right) \left(\frac{c_{xy}}{h}\right)_o^* - (\tilde{G}_o h_o^2 - \tilde{\alpha}_o) \left(\frac{c_{xy}}{h}\right)_o \end{aligned} \quad (56)$$

for $o = l/r$. Now, the case $b = 0$ is trivially satisfied since $(c_{xy}/h)_o^* = (c_{xy}/h)_o$. Otherwise, when $b \neq 0$, for c_{\parallel} given the closed q_1 subsystem can be solved so that h_o^* is also fixed, and (56) amounts to controlling the sign of a quadratic polynomial function of $(c_{xy}/h)_o^*$ through a and c_{\perp} . So, if we ensure

$$1 + \tilde{G}_o(h_o^*)^4 - 2\tilde{\alpha}_o(h_o^*)^2 < 0 \Leftrightarrow \frac{1}{(h_o^*)^2} + \tilde{G}_o(h_o^*)^2 < 2\tilde{\alpha}_o \equiv 2\left(\frac{c_{xx}}{h^2}\right)_o \frac{1}{a^2}$$

with a small enough and if we next choose $(c_{xy}/h)_o^*$ large enough (in magnitude) simply by controlling c_{\perp} (it suffices to choose $c_{\parallel}^2 - c_{\perp}^2 > 0$ small enough, given c_{\parallel} , b and a) then (56) holds, thus (50).

Condition (51) can also be analyzed similarly to (49) and (50) on noting (44). Recalling the Riemann invariants for c_{-1} and c_1 , it suffices that for $o = l/r$

$$\begin{aligned} \left(e_{\perp} - \frac{P_{\perp}^2}{2c_{\perp}^2} \right) (q_o^{\sharp}) - \left(\hat{e}_{\perp} - \frac{\pi_{\perp}^2}{2c_{\perp}^2} \right)_o^* \\ + P_{\perp}(q_o^{\sharp}) \left(\frac{P_{\perp}(q_o^{\sharp}) - (\pi_{\perp})_o^*}{c_{\perp}^2} - \left(\frac{c_{xy}}{a^2 h} \right)_o^{\sharp} + \left(\frac{c_{xy}}{a^2 h} \right)_o^* \right) \leq 0 \end{aligned} \quad (57)$$

holds. With $e_{\perp}(c_{xy}/h) = G(h^2/c_{xx})(c_{xy}/h)^2/2$ and $P_{\perp}(c_{xy}/h) = Gh^2(c_{xy}/h)$, note that the LHS in (57) is a quadratic polynomial in $(\frac{c_{xy}}{h})_o^{\sharp}$

$$\begin{aligned} \left(1 + \hat{G}_o - 2c_{xx}/a^2 \right) \left(\left(\frac{c_{xy}}{h} \right)_o^{\sharp} \right)^2 - \left(\frac{2c_{xx}}{Gh^2} \right)_o^* \left(\hat{e}_{\perp} - \frac{\pi_{\perp}^2}{2c_{\perp}^2} \right)_o^* \\ + 2c_{xx} \left(\frac{1}{a^2} \frac{c_{xy}}{h} - \frac{\pi_{\perp}}{c_{\perp}^2} \right)_o^* \left(\frac{c_{xy}}{h} \right)_o^{\sharp} \leq 0 \end{aligned} \quad (58)$$

where $\hat{G}_o := \left(\frac{Gh^2 c_{xx}}{c_{\perp}^2} \right)_o^*$. Now, to ensure condition (57) similarly to (55) i.e.

$$\left(1 + \hat{G}_o - 2c_{xx}/a^2 \right)_o^* < 0 \Leftrightarrow c_{\perp}^2 + G(c_{xx}h^2)_o^* \leq \frac{2(c_{xx})_o^* c_{\perp}^2}{a^2}$$

one cannot anymore choose a and $c_{\parallel}^2 - c_{\perp}^2 > 0$ independently small. But (57) can still be satisfied under the more stringent condition

$$\frac{a^2}{c_{\perp}^2} \leq \frac{2(c_{xx})_o^*}{c_{\parallel}^2 + G(h^2 c_{xx})_o^*} \leq \frac{2(c_{xx})_o^*}{c_{\perp}^2 + G(h^2 c_{xx})_o^*}$$

plus simultaneously a large enough $(c_{xy}/h)_o^{\sharp}$ (in magnitude).

If $b(u^* - u_o) \neq 0$ then one can again ensure a large enough $(c_{xy}/h)_o^{\sharp}$ with $c_{\parallel}^2 - c_{\perp}^2 > 0$ small, which is obviously compatible with our requirements for condition (55).

If $b(u^* - u_o) = 0$, then (51) simplifies and reads

$$\begin{aligned} \frac{G}{2} \left(\frac{h^2}{c_{xx}} \right)_o^* \left(\left| \frac{c_{xy}}{h} \right|_{\sharp,o}^2 - \left| \frac{c_{xy}}{h} \right|_o^2 \right) \leq \frac{G(h_o^*)^2}{a^2} \left(\frac{c_{xy}}{h} \right)_{\sharp,o} \left(\left(\frac{c_{xy}}{h} \right)_{\sharp,o} - \left(\frac{c_{xy}}{h} \right)_o \right) \\ - \frac{\left(G(h_o^*)^2 \left(\frac{c_{xy}}{h} \right)_{\sharp,o} - Gh_o^2 \left(\frac{c_{xy}}{h} \right)_o \right)^2}{2c_{\perp}^2} \end{aligned} \quad (59)$$

which is satisfied if c_{\perp}^2 is large enough. Now, recalling the constraint above on $c_{\perp}^2/c_{\parallel}^2 < 1$, this requires one to increase c_{\parallel} . So an entropy-consistent choice for the relaxation parameters can always be identified by a simple algorithm explained in the next Section 3.4 with the whole computational scheme.

In the end, we note that the parameter $b = 2Gh^2 c_{xy}$, which has no sign a priori, can be chosen “freely”. To minimize numerical diffusion, we compute it as the solution to $\partial_t b + u \partial_x b = 0$ initialized consistently with its definition.

3.4 Numerical schemes for SVTM and SVUCM

Finally, let us summarize our numerical scheme to simulate SVTM, which turns out to be useful for SVUCM at the cost of very few modifications.

But first, for each Riemann problem, we propose to also “relax” a , c_{\parallel} and c_{\perp} as independent variables solutions to pure transport equations, similarly to b , for the sake of more precision. Then, the exact values of the intermediate states change, and become a function of *left and right* parameter values. For SVTM 1D Riemann problems, they become:

$$\begin{aligned}
u^* &= \frac{c_{\parallel,l}u_l + \pi_{\parallel,l} + c_{\parallel,r}u_r - \pi_{\parallel,r}}{c_{\parallel,l} + c_{\parallel,r}}, & \pi_{\parallel}^* &= \frac{c_{\parallel,r}(\pi_{\parallel,l} + c_{\parallel,l}u_l) + c_{\parallel,l}(\pi_{\parallel,r} - c_{\parallel,r}u_r)}{c_{\parallel,l} + c_{\parallel,r}}, \\
\frac{1}{h_{\parallel,l}^*} &= \frac{1}{h_{\parallel,l}} + \frac{c_{\parallel,r}(u_r - u_l) + \pi_{\parallel,l} - \pi_{\parallel,r}}{c_{\parallel,l}(c_{\parallel,l} + c_{\parallel,r})}, & \frac{1}{h_{\parallel,r}^*} &= \frac{1}{h_{\parallel,r}} + \frac{c_{\parallel,l}(u_r - u_l) + \pi_{\parallel,r} - \pi_{\parallel,l}}{c_{\parallel,r}(c_{\parallel,l} + c_{\parallel,r})}, \\
v_l^* &= v_l + \frac{b_l}{c_{\perp,l}^2 - c_{\parallel,l}^2} \frac{c_{\parallel,r}(u_l - u_r) + \pi_{\parallel,r} - \pi_{\parallel,l}}{c_{\parallel,l} + c_{\parallel,r}}, & v_r^* &= v_r + \frac{b_r}{c_{\perp,r}^2 - c_{\parallel,r}^2} \frac{c_{\parallel,l}(u_r - u_l) + \pi_{\parallel,l} - \pi_{\parallel,r}}{c_{\parallel,l} + c_{\parallel,r}}, \\
\pi_{\perp,l}^* &= \pi_{\perp,l} - \frac{b_l c_{\parallel,l}}{c_{\perp,l}^2 - c_{\parallel,l}^2} \frac{c_{\parallel,r}(u_l - u_r) + \pi_{\parallel,r} - \pi_{\parallel,l}}{c_{\parallel,l} + c_{\parallel,r}}, & \pi_{\perp,r}^* &= \pi_{\perp,r} + \frac{b_r c_{\parallel,r}}{c_{\perp,r}^2 - c_{\parallel,r}^2} \frac{c_{\parallel,l}(u_r - u_l) + \pi_{\parallel,l} - \pi_{\parallel,r}}{c_{\parallel,l} + c_{\parallel,r}}, \\
\left(\frac{c_{xy}}{h}\right)_l^* &= \left(\frac{c_{xy}}{h}\right)_l - \frac{a_l^2 b_l / c_{\parallel,l}}{c_{\perp,l}^2 - c_{\parallel,l}^2} \frac{c_{\parallel,r}(u_l - u_r) + \pi_{\parallel,r} - \pi_{\parallel,l}}{c_{\parallel,l} + c_{\parallel,r}}, & \left(\frac{c_{xy}}{h}\right)_r^* &= \left(\frac{c_{xy}}{h}\right)_r + \frac{a_r^2 b_r / c_{\parallel,r}}{c_{\perp,r}^2 - c_{\parallel,r}^2} \frac{c_{\parallel,l}(u_r - u_l) + \pi_{\parallel,l} - \pi_{\parallel,r}}{c_{\parallel,l} + c_{\parallel,r}}, \\
v_{\#} &= \frac{c_{\perp,l}v_l^* + \pi_{\perp,l}^* + c_{\perp,r}v_r^* - \pi_{\perp,r}^*}{c_{\perp,l} + c_{\perp,r}}, & \pi_{\#} &= \frac{c_{\perp,r}(\pi_{\perp,l}^* + c_{\perp,l}v_l^*) + c_{\perp,l}(\pi_{\perp,r}^* - c_{\perp,r}v_r^*)}{c_{\perp,l} + c_{\perp,r}}, \\
\left(\frac{c_{xy}}{h}\right)_r^{\#} &= \left(\frac{c_{xy}}{h}\right)_r^* + \frac{a_r^2}{c_{\perp,r}^2} \frac{c_{\perp,r}c_{\perp,l}(v_l^* - v_r^*) + c_{\perp,l}(\pi_{\perp,l}^* - \pi_{\perp,r}^*)}{c_{\perp,l} + c_{\perp,r}}, & \left(\frac{c_{xy}}{h}\right)_l^{\#} &= \left(\frac{c_{xy}}{h}\right)_l^* + \frac{a_l^2}{c_{\perp,l}^2} \frac{c_{\perp,l}c_{\perp,r}(v_r^* - v_l^*) + c_{\perp,r}(\pi_{\perp,r}^* - \pi_{\perp,l}^*)}{c_{\perp,l} + c_{\perp,r}}, \\
(h^{-2}c_{xx})_l^* &= (h^{-2}c_{xx})_l^{\#} = h^{-2}c_{xx} & (h^{-2}c_{xx})_r^* &= (h^{-2}c_{xx})_r^{\#} = h^{-2}c_{xx} \\
(h^2c_{zz})_l^* &= (h^2c_{zz})_l^{\#} = h^2c_{zz} & (h^2c_{zz})_r^* &= (h^2c_{zz})_r^{\#} = h^2c_{zz}
\end{aligned} \tag{60}$$

however the conditions (49–50–51) do not change, and our discussion in Section 3.3 to achieve discrete entropy dissipation by well-chosen a , c_{\parallel} and c_{\perp} is still valid (although the identification of numerical values for the right and left relaxation parameters may become more difficult).

Second, to use a similar approach for SVUCM, note also that (36) becomes

$$\left\{ \begin{aligned} & \partial_t h + \partial_x(hu) = 0 \\ & \partial_t(hu) + \partial_x(hu^2) + \partial_x(gh^2/2) + \partial_x(Gh(c_{zz} - c_{xx})) = 0 \\ & \partial_t(h^2c_{xx}) + u\partial_x(h^2c_{xx}) = 0 \\ & \partial_t(h^{-2}c_{zz}) + u\partial_x(h^{-2}c_{zz}) = 0 \\ & \partial_t(c_{yy} - c_{xy}^2/c_{xx}) + u\partial_x(c_{yy} - c_{xy}^2/c_{xx}) = 0 \\ & \partial_t(hv) + \partial_x(huv) - \partial_x(Ghc_{xy}) = 0 \\ & \partial_t(hc_{xy}) + u\partial_x(hc_{xy}) - hc_{xx}\partial_x v = 0 \end{aligned} \right. \tag{61}$$

while the pressures associated with the energy contributions E_{\parallel} and E_{\perp} , which are exactly the same as in SVTM, then respectively read $P_{\parallel} = \frac{gh^2}{2} + Gh(c_{zz} - c_{xx})$ and $P_{\perp} = -Ghc_{xy}$. Now, the pressures follow similar evolution equations for smooth solutions with parameters $c_{\parallel}^2 = h^2(gh + G(3c_{zz} + c_{xx}))$, $c_{\perp}^2 = Gh^2c_{xx}$, $b \equiv 0$, and this is why we can use the same (pseudo-)relaxation approach. For SVUCM, we define as Riemann solver the (exact) solution to the following

linearly degenerate system

$$\left\{ \begin{array}{l} \partial_t h - \partial_x(hu) = 0 \\ \partial_t(hu) + \partial_x(hu^2 + \pi_{\parallel}) = 0 \\ \partial_t(h\pi_{\parallel}) + \partial_x(hu\pi_{\parallel}) + c_{\parallel}^2 \partial_x u = 0 \\ \partial_t(-h^2 c_{xy}) + \partial_x(-h^2 u c_{xy}) + a^2 \partial_x v = 0 \\ \partial_t(hv) + \partial_x(huv + \pi_{\perp}) = 0 \\ \partial_t(h\pi_{\perp}) + \partial_x(hu\pi_{\perp}) + c_{\perp}^2 \partial_x v = 0 \\ \partial_t(h^{-1} c_{zz}) + \partial_x(h^{-1} c_{zz} u) = 0 \\ \partial_t(h^3 c_{xx}) + \partial_t(h^3 c_{xx} u) = 0 \\ \partial_t(h(c_{yy} - c_{xy}^2/c_{xx})) + \partial_x(h(c_{yy} - c_{xy}^2/c_{xx})u) = 0 \end{array} \right. \quad (62)$$

which is easily deduced from (62) on noting the new value of $a^2 = c_{xx}h^2$ that is consistent with its definition in smooth cases.

As opposed to SVTM, it always holds $b = 0$ in the SVUCM case. This is consistent with the fact that there is no non-conservative product between nonlinear fields in (61) as opposed to (36) (observe indeed that the subsystem for q_1 is closed in SVUCM, like in SVTM, and that for $q_2 = (c_{xy}, v, c_{yy})$ is also closed – unlike SVTM). Then, as a consequence, entropy-consistency can be ensured for SVUCM following the same approach as for SVTM !

In fact, since $b = 0$, only the two conditions (49) and (51) have to be checked. The first one is still satisfied with the choice in [10]. The second reads

$$\begin{aligned} \frac{G}{2} \left(\frac{1}{h^2 c_{xx}} \right)_o^* \left(|hc_{xy}|_{\sharp,o}^2 - |hc_{xy}|_o^2 \right) &\leq \frac{G}{a^2} (hc_{xy})_{\sharp,o} \left((hc_{xy})_{\sharp,o} - (hc_{xy})_o \right) \\ &\quad - \frac{G}{2c_{\perp}^2} \left((hc_{xy})_{\sharp,o} - (hc_{xy})_o \right)^2 \end{aligned} \quad (63)$$

since $b = 0$ and is always satisfied when $a^2 \leq c_{xx}h^2$ (unlike (59) in SVTM).

Now, given a polygonal mesh of \mathbb{R}^2 , with cells V_i and interfaces Γ_{ij} , time evolutions of viscoelastic flows can be numerically simulated using a piecewise-constant state vector

$$q := (H, HU, HV, HC_{xx}, HC_{yy}, HC_{xy}/\sqrt{C_{xx}C_{yy}}, HC_{zz})$$

with convex admissible domain

$$\{H, HC_{xx}, HC_{yy}, HC_{zz} > 0 ; \quad -H < HC_{xy}/\sqrt{C_{xx}C_{yy}} < H\},$$

that is a Finite-Volume (FV) approximation either for SVTM or for SVUCM.

Time-discrete sequences can be computed in two sub-steps. First, define $q_i^{n+1,-}$ in (17) with a numerical flux of the form (18–19) using the 1D Riemann solver R defined by (60) for SVTM, and the straightforward modification proposed above for SVUCM. Second, compute (30), (31) and (32).

Proposition 3.4. *At each time step, there exist left and right initial states of the relaxation parameters c_{\parallel} , c_{\perp} and b for all Riemann problems at interfaces Γ_{ij} such that the convex admissible domain for q is preserved, and the second-principle formulation (33) is satisfied under the stringent CFL condition (22).*

In practice, we need *numerical values* of relaxation parameters such that conditions (49) and (51) hold, plus (50) for SVTM: they are useful in (60). An adequate choice of the relaxation parameters can be computed in each Riemann problem as follows, for instance.

First, initialize c_{\parallel} to ensure (49) like [10] for 1D cases

$$c_{\parallel,l} = h_{\parallel,l} \left(\sqrt{\partial_h P_{\parallel}(q_l)} + 2 \left((u_l - u_r)_+ + \frac{(\pi_{\parallel,r} - \pi_{\parallel,l})_+}{h_{\parallel,l} \sqrt{\partial_h P_{\parallel}(q_l)} + h_{\parallel,r} \sqrt{\partial_h P_{\parallel}(q_r)}} \right) \right), \quad (64)$$

$$c_{\parallel,r} = h_{\parallel,r} \left(\sqrt{\partial_h P_{\parallel}(q_r)} + 2 \left((u_l - u_r)_+ + \frac{(\pi_{\parallel,l} - \pi_{\parallel,r})_+}{h_{\parallel,l} \sqrt{\partial_h P_{\parallel}(q_l)} + h_{\parallel,r} \sqrt{\partial_h P_{\parallel}(q_r)}} \right) \right). \quad (65)$$

where we denoted $\partial_h P_{\parallel}(q_o) = \partial_h|_{hc_{xx}^{-1/2}, hc_{zz}^{+1/2}} P_{\parallel}(q_o) = gh_o + G(3c_{xx} + c_{zz})_o$.

Given $c_{\parallel,o}$, only $a_o^2 = c_{xx,o} h_o^2$ remains to compute for SVUCM, while

$$a_o^2 = c_{xx,o} \wedge r_o^0 \frac{2c_{xx,o}^*}{1 + Gh_o^2 c_{xx,o} / c_{\parallel,o}^2}$$

for SVTM is not enough.

For SVTM, one still needs to compute $c_{\perp,o}^2 = r_o^n c_{\parallel,o}^2$ after n iterations of a strictly increasing sequence $r_o^n < r_o^{n+1} \leq 1$ with limit 1 starting from $r_o^0 = Gh_o^2 c_{xx,o} / c_{\parallel,o}^2 > 0$ until (50) (or the weaker conditions (49)+(50)) are satisfied for some n both for $o = l/r$ simultaneously. Moreover, given $c_{\parallel,o}^2, a_o^2, b_o = 2Gh_o^2 c_{xy,o}$ and $c_{\perp,o}^2 / c_{\parallel,o}^2 = r_o^n \leq 1$, one still has to inspect (51) in SVTM case. If $b_o(u_o - u^*) \neq 0$ we iterate further on the sequence $r_o^n < r_o^{n+1} \leq 1$ defining $c_{\perp,o}^2$ until (51) are satisfied for some n both for $o = l/r$ simultaneously. Otherwise, if $b_o(u_o - u^*) = 0$ for any $o = l/r$, then $c_{\parallel,o}$ has to be increased where (51) is not satisfied: one can use some unbounded increasing sequence \tilde{r}_n and iterate on n to define $c_{\parallel,o}$ starting with (64–65).

Finally, using the analytical Riemann solution of section 3.2 one has

$$\begin{aligned} \frac{1}{\tau^n} \int_{-\left(\sum_j \frac{|\Gamma_{ij}|}{|V_i|}\right)^{-1}}^0 R(x/\tau^n, q_l, q_r) dx &= (\xi_{-2,-} + \bar{s}_i^n) q_l + (\xi_{-1,-} - \xi_{-2,-}) q_l^* \\ &+ (\xi_{0,-} - \xi_{-1,-}) q_l^{\sharp} + (\xi_{1,-} - \xi_{0,-}) q_r^{\sharp} + (\xi_{2,-} - \xi_{1,-}) q_r^* + (-\xi_{2,-}) q_r \\ &= \bar{s}_i^n q_l + (\xi_{-1,-} - \xi_{-2,-}) (q_l^* - q_l) + (\xi_{0,-} - \xi_{-1,-}) (q_l^{\sharp} - q_l) \\ &+ (\xi_{1,-} - \xi_{0,-}) (q_r^{\sharp} - q_l) + (\xi_{2,-} - \xi_{1,-}) (q_r^* - q_l) + (-\xi_{2,-}) (q_r - q_l) \end{aligned} \quad (66)$$

where we have denoted $x_- = \min(x, 0)$ the non-positive part of a real number x and $\bar{s}_i^n := \frac{1}{\tau^n} \left(\sum_j \frac{|\Gamma_{ij}|}{|V_i|} \right)^{-1} \geq s_i^n > 0$. Note that (66) is consistent with conservation laws for “conservative” components of variable q like U i.e.

$$\mathbf{F}_{i \rightarrow j}^U(q_i, q_j; \mathbf{n}_{i \rightarrow j}) + \mathbf{F}_{j \rightarrow i}^U(q_j, q_i; \mathbf{n}_{j \rightarrow i}) = 0.$$

Therefore, under our stringent CFL condition (22), (23) rewrites

$$\begin{aligned}
q_i^{n+1,-} &= \sum_j \frac{|\Gamma_{ij}|}{|V_i|} \mathbf{O}_{i,j} \int_{-\left(\sum_j \frac{|\Gamma_{ij}|}{|V_i|}\right)^{-1}}^0 R(x/\tau^n, \mathbf{O}_{i,j}^{-1} q_i^n, \mathbf{O}_{i,j}^{-1} q_j^n) dx \\
&= q_i^n + \tau^n \sum_j \frac{|\Gamma_{ij}|}{|V_i|} \left((\xi_{-1,-} - \xi_{-2,-}) (\mathbf{O}_{i,j} q_l^* - q_i^n) \right. \\
&\quad + (\xi_{0,-} - \xi_{-1,-}) (\mathbf{O}_{i,j} q_l^\# - q_i^n) + (\xi_{1,-} - \xi_{0,-}) (\mathbf{O}_{i,j} q_r^\# - q_i^n) \\
&\quad \left. + (\xi_{2,-} - \xi_{1,-}) (\mathbf{O}_{i,j} q_r^* - q_i^n) + (-\xi_{2,-}) (q_j^n - q_i^n) \right) \quad (67)
\end{aligned}$$

where $q_o^{(*,\#)}$ are the intermediate states of the Riemann solver $R(\xi, \mathbf{O}_{i,j}^{-1} q_i^n, \mathbf{O}_{i,j}^{-1} q_j^n)$, $\xi_{-2} < \xi_{-1} < \xi_0 < \xi_{+1} < \xi_{+2}$ its wave speeds, and where τ^n can be computed at each time step after all Riemann problems at all faces to satisfy (22).

4 Numerical illustration and discussion

We now illustrate the SVTM and SVUCM models using numerical solutions computed with our FV schemes in benchmark test cases.

4.1 Stoker test case

This is a well-known benchmark test case for the (time-dependent, inviscid) Saint-Venant shallow-water equations, which models an idealized *dam-break* (i.e. the propagation under gravity of a shock wave in a finite-depth fluid initially at rest) [42]. A solution for $t \in (0, .2)$ is computed in a square $(x, y) \in [0, 1]^2$ starting from the initial condition

$$(H, U, V, C_{xx}, C_{yy}, C_{xy}, C_{zz}) = \begin{cases} (3, 0, 0, 1, 1, 0, 1) & x + y < 1 \\ (1, 0, 0, 1, 1, 0, 1) & x + y > 1 \end{cases}$$

that consists in two equilibrium rest states on each side of the line $x + y = 1$. For the boundary conditions, we use the “ghost cell” method (see e.g. [29]) assuming translation invariance along $x + y$ isolines.

The main point of Stoker test case is usually to compare the speed of the shock front with observations (the solution expected – numerically at least – is indeed a free-shear flow). Alternatively, assuming translation invariance along $x + y$ isolines, this is a 1D Riemann problem that uniquely determines q_1 (as well as q_2 for SVUCM). So the test case can be used to accurately understand the new variable \mathbf{C} in out-of-equilibrium dynamics, phenomenologically at least, as a function of the viscoelastic parameters G, λ .

Moreover, for benchmarking purposes, we also aim at comparing the new 2D scheme with former 1D numerical results obtained along $x = y$ in our previous work [10] for the subsystem q_1 of SVUCM model, at Froude number $g^{-1/2} = .3$ ($g = 10$), elasticity number $G = 10$ and Weissenberg number $\lambda = 1$. This of course assumes that our 2D scheme converges to a translation-invariant solution.

In Fig. 2, this is exactly what we observe, see e.g. the variable H in Fig.1 (note that translation-invariance is used to define the values of “ghost cells” in

Riemann problems at boundary faces). We compare results obtained with 2D Cartesian meshes of $(2^5 + 1) = 1089$, $(2^6 + 1) = 4225$ cells and 1D regular grids with $2^8 + 1 = 257$ and $2^9 + 1 = 513$ cells. The 2D solutions seem to preserve the initial translation invariance and converge to the (unique) 1D translation-invariant solution. (The positions of the fronts seem already quite well resolved with our coarse mesh, at least, although the 2D state values are only 10% accurate relatively to 1D.)

For benchmarking purposes, the test case also allows one to compare SVTM and SVUCM in a simple configuration. We do not observe significant differences for H, U at such short times, however the non-zero stress components Σ_{nn}, Σ_{zz} are not the same (although they have similar tendencies) see Fig. 3 for the various 1D (converged) values.

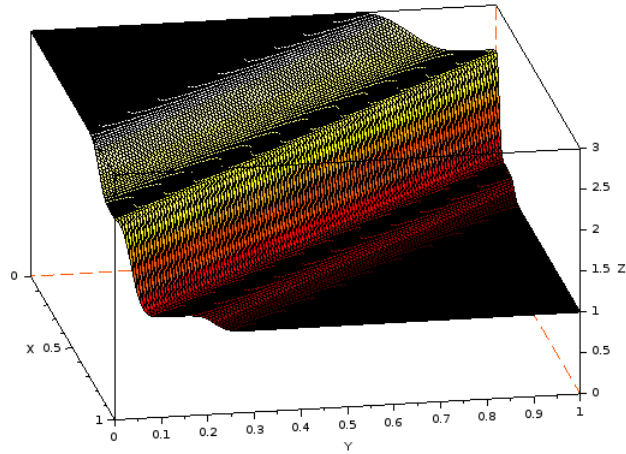


Figure 1: Stoker test case: flow depth $H(x, y)$ at final time $T = .2$

Last, variations in the parameters G and λ can also be well understood phenomenologically (from the viscoelastic physics viewpoint) in the present 1D test case. Since analyzing variations in the parameters G and λ was already done in [10] for SVUCM, we concentrate here on SVTM.

In Fig. 4 we show H, C_{xx}, C_{zz} for SVTM at $T = .2$ when $G = .1, 1, 10$ and $\lambda = .01, .1, 1$. Increasing G at fixed λ only slightly increases the speeds of the genuinely nonlinear waves, while it more essentially increases the jump in H at the linearly degenerate wave (a contact discontinuity) and decreases the jumps in C_{xx}, C_{zz} . This is physically coherent with the fact that the elasticity G controls how difficult it is to locally deform the fluid materials of depth H , and connecting two equilibria at $H = 3$ and $H = 1$ through deformations becomes harder as G increases. However, if λ simultaneously decreases, then variations in space of the strain C_{xx}, C_{zz} are fast smoothed back to equilibrium and a viscous profile arises (see $G = 10, \lambda = 10^{-2}$ in Fig. 4). We recall that *both* models SVUCM and SVTM formally converge to the viscous Saint-Venant equations in asymptotics $\lambda, G^{-1} \rightarrow 0$ where $1/G\lambda$ remains bounded and defines a Reynolds number. Of

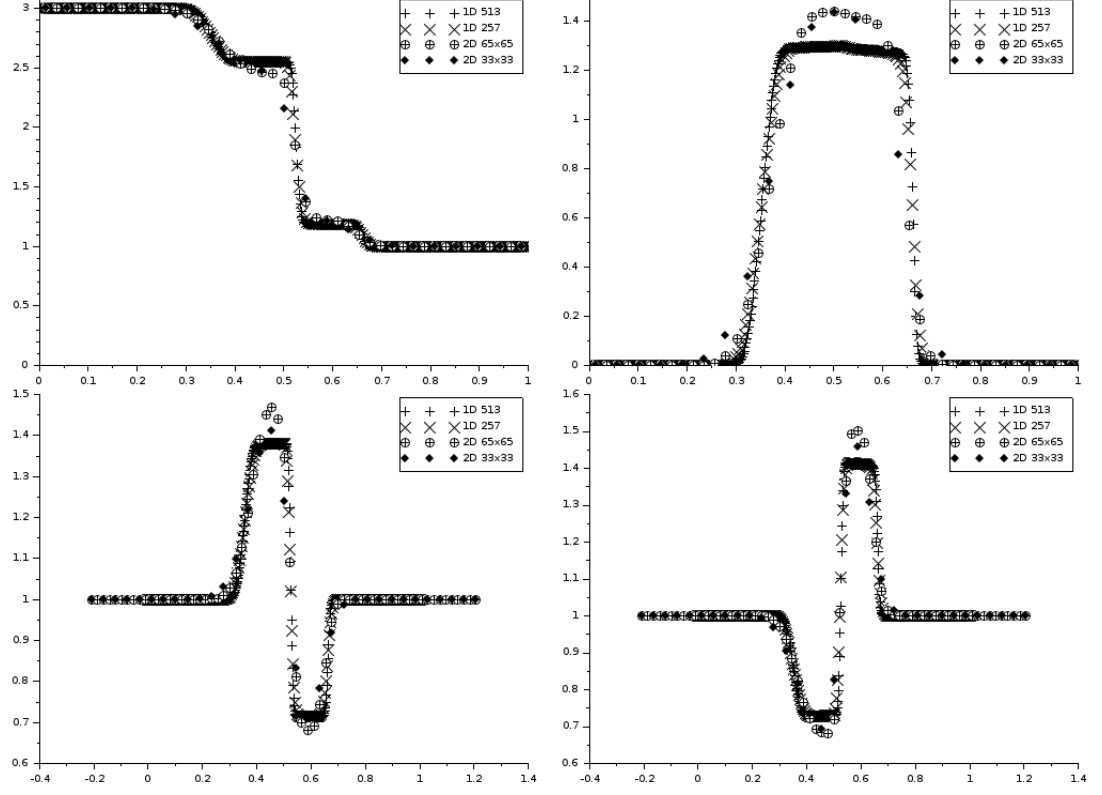


Figure 2: Stoker test case: $H, U \cdot n, C_{nn}, C_{zz}$ computed by SVUCM 2D (cross-section $x = y$) and 1D (along \mathbf{n} normal to the initial discontinuity at $x + y = 1$)

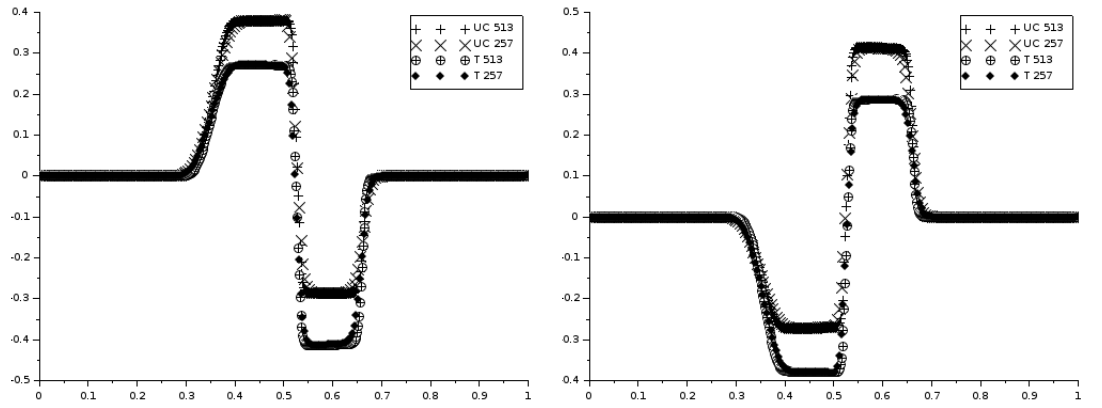


Figure 3: Stoker test case: Σ_{nn}, Σ_{zz} (left/right) for SVTM and SVUCM (T/UC) along the normal \mathbf{n} to the initial discontinuity at $x + y = 1$ (in G units).

course, at fixed parameter values, it is not so clear to define how close solutions are from a viscous approximation, all the less when the Froude number $g^{-1/2}$ also varies. This may be an interesting direction for future research directions, insofar as $g^{-1/2}$ should be quite low in real viscoelastic fluids.

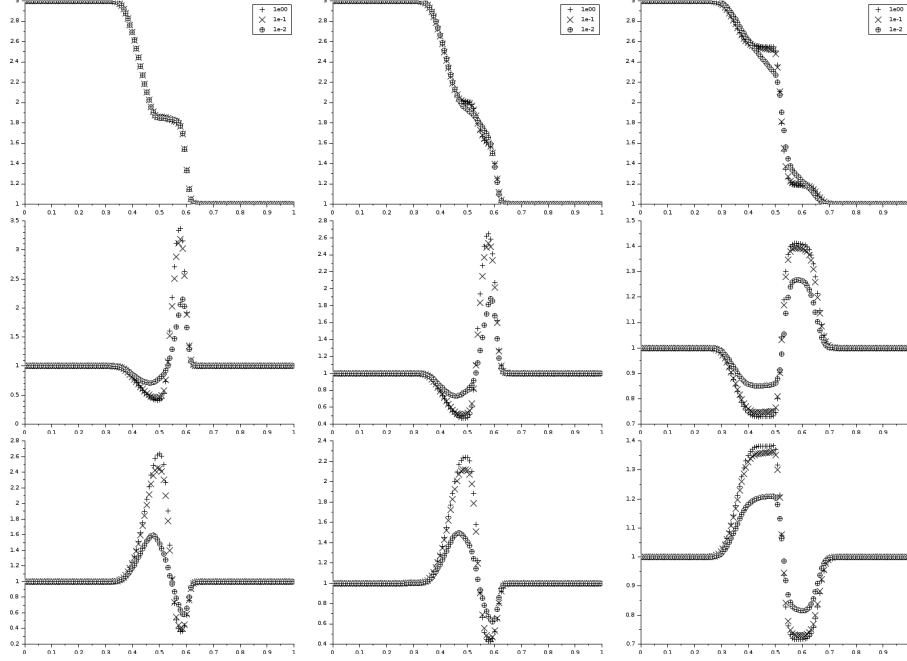


Figure 4: Stoker test case: H (top), C_{xx} (middle), C_{zz} (bottom) at $T = .2$ for $\lambda = .01, .1, 1$ when $G = .1, 1, 10$ (left, center and right) with 257 cells.

4.2 Collapse of a column

To emphasize the 2D character of the SVTM and SVUCM models, we now consider a cylindrical version of Stoker test case, which models the idealized collapse of a fluid column. A solution for $t \in (0, .2)$ is computed in a square $(x, y) \in [0, 1]^2$ starting from the initial condition

$$(H, U, V, C_{xx}, C_{yy}, C_{xy}, C_{zz}) = \begin{cases} (3, 0, 0, 1, 1, 0, 1) & (x - .5)^2 + (y - .5)^2 < .2 \\ (1, 0, 0, 1, 1, 0, 1) & (x - .5)^2 + (y - .5)^2 > .2 \end{cases}$$

see Fig.6. Note that, a priori, no boundary condition is needed here if we assume our computational domain is a fictitious truncation of the plane \mathbb{R}^2 with fictitious boundaries far enough from the initial (circular) discontinuity.

The main goal of that testcase is usually to see the impact of diverging gravity currents on axisymmetric initial conditions.

Here, we keep the Froude number moderately small $g^{-1/2} = .3$ as before, and we study the influence of the elasticity modulus G for SVTM and SCUVM at a final time $T = .2$. Note that we can choose the Weissenberg number arbitrarily large, and the influence of the relaxation-to-equilibrium term is negligible with

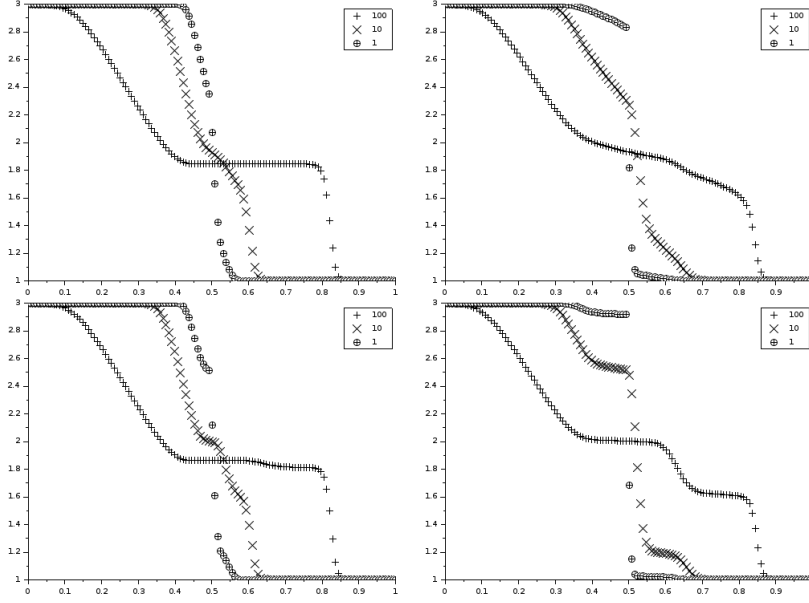


Figure 5: Stoker test case: H at $T = .2$ for $g = 1, 10, 100$ when $\lambda = .01, 1$ (top/bottom) and $G = 1, 10$ (left/right) with 257 cells.

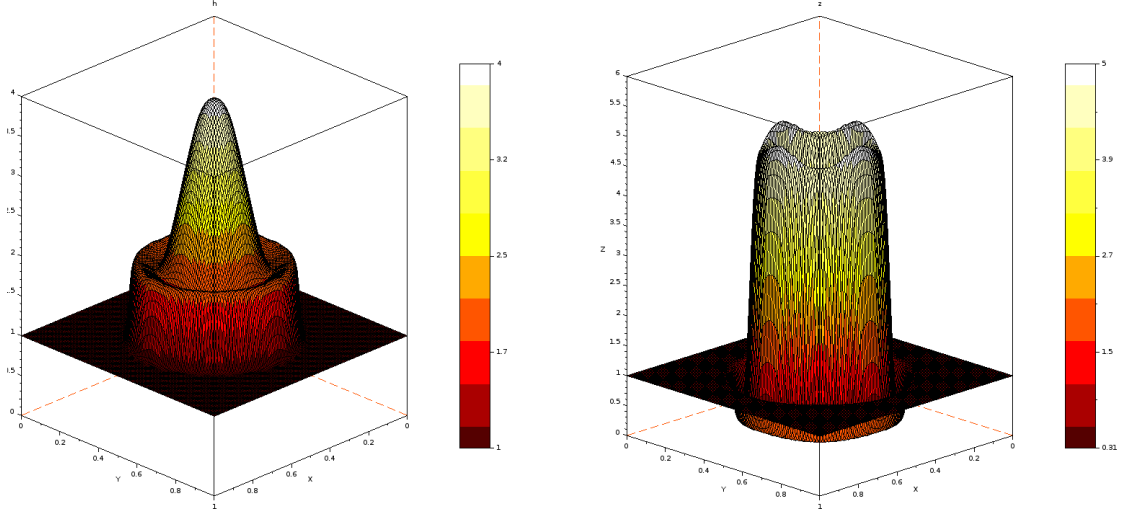


Figure 6: Column test case: H, Σ_{zz} at final time $T = .2$ with a large Weissenberg number $\lambda = 1$

$\lambda = 1 \gg T$ for instance. Comparing the usual hydrodynamical quantities $H, \mathbf{U} \cdot \mathbf{n}$ along cross-section $x = y$, there is little difference between SVTM and SCUVM for the same values G . At large $G = 1$, the additional wave clearly shows up in H both for SVTM and SVUCM, as opposed to the small $G = .001$ case, close to the usual Saint-Venant shallow-water model as expected, see Fig. 7.

Now, we can also compare $\mathbf{C} - \mathbf{I}$ in SVUCM with $\mathbf{I} - \mathbf{C}$ in SVTM. It is then quite striking that the strain deviation from equilibrium (hence the stress) is more important for *horizontal* components in SVUCM, see the – most important – radial component $\mathbf{C}\mathbf{n} \cdot \mathbf{n} - 1 = \frac{1}{G}\Sigma\mathbf{n} \cdot \mathbf{n}$ in Fig. 7, and for *vertical* component $C_{zz} - 1 = \frac{1}{G}\Sigma_{zz}$ in SVTM. The strain discrepancies in between SVTM and SVUCM should be investigated in the future, in particular to compare with more standard viscoelastic flow settings with a low Froude number and *shear* forcing that generates some numerical instabilities in the stress variable (see HWNP below in Section 4.3).

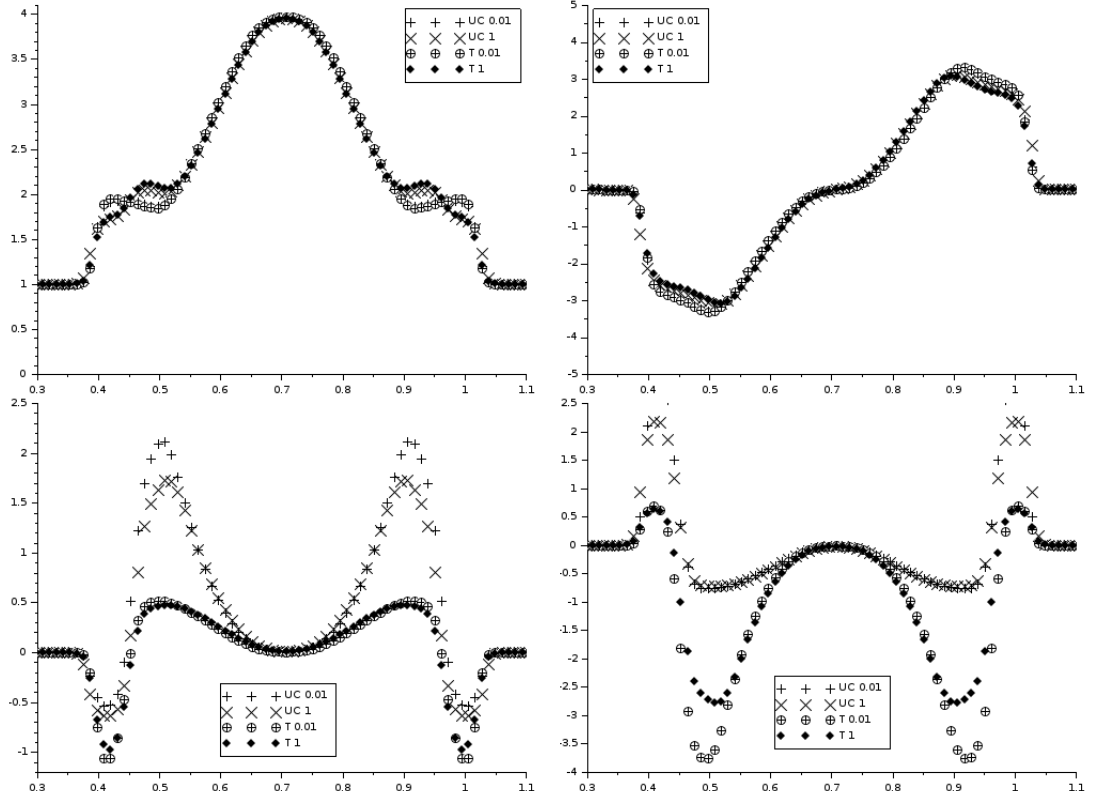


Figure 7: Column test case: $H, \mathbf{U} \cdot \mathbf{n}, \Sigma\mathbf{n} \cdot \mathbf{n}, \Sigma_{zz}$ along diagonal $y = x$ with unit normal \mathbf{n} , for SVTM and SVUCM with elasticity $G = 1$ and $G = .01$, at final time $T = .2$ with a large Weissenberg number $\lambda = 1$ (stresses are in G units)

4.3 Lid-driven cavity

We finally consider a well-known test case for viscous (and viscoelastic) fluid models that involves *stationary* solutions. It aims at computing, in a closed

square box $(x, y) \in [0, 1]^2$ with impermeable walls, a steady flow satisfying no-slip boundary conditions (i.e. $u = 0 = v$) at $x = 0$, $x = 1$, $y = 0$ and at $y = 1$ typically $u = 1$, $v = 0$ (or a regularized version, see e.g. [41]).

When benchmarking time-dependent (evolutionary) models, stationary solutions are usually computed for large times in the hope it becomes close to a limit fixed by the data.

For viscoelastic fluids however, numerous computer simulations of incompressible creeping flows of Maxwell fluids encounter numerical instabilities when elastic stresses increase, see the review about the lid-driven cavity case in [41].

Precisely, discretizations do not converge to a stationary solution at large Weissenberg number values. This is one manifestation of the so-called High-Weissenberg-Number-Problem (HWNP).

Various reasons have been invoked to explain the HWNP. For instance, numerical instabilities may appear when the models do not have unique solutions anymore. Now, non-uniqueness may in fact be natural. Instabilities, i.e. persistent large fluctuations in experimental measures, are also sometimes observed physically in settings with (apparently) steady conditions, see e.g. the references in [41] as concerns cavity experiments. But it is not completely clear why the sensitivity of a mathematical model that idealizes the physics should exactly correspond to the sensitivity of an experimental set-up (unless the model is very good at describing all the physics, and its numerical approximation is very accurate). Indeed, numerical instabilities could also be of a purely mathematical nature, and then possibly indicate some imperfection of the (numerical) model at describing the physics, in fact.

That is why, although our aim in the present work is not to “solve” the HWNP, we nevertheless think it is interesting to simulate our new numerical models in more usual conditions for viscoelastic flows such as the lid-driven cavity, where a HWNP occurs for most existing models. Indeed, our models somehow enlarge the physical regimes that are usually accessible to (numerical) viscoelastic flows, with a vanishing retardation-time and a non-zero Froude number.

First, to obtain conditions that are more usual for viscoelastic flows in a lid-driven cavity, we choose a low Froude number $g^{-1/2} = 10^{-3/2}$ ($g = 10^3$), to get closer to the incompressible limit. Next, we add a viscous component to the stress, with a so-called “solvent viscosity” $\nu_s = 10^{-1}$. Although this does not exactly produce creeping flows like in most viscoelastic testcases (our model is evolutionary), the Reynolds number remains quite small $\nu_s^{-1} = 10$ so the boundary influence is not negligible.

We compute solutions at large times for various values of G and λ .

In Fig. 8, we compare at $T = 1$ standard quantities of interest (U along $x = .5$, V along $y = .5 \dots$) computed with a relatively coarse Cartesian mesh of $33 \times 33 = 1089$ cells. First, whereas H , U and V are hardly different for SVTM and SVUCM, the viscoelastic stress are different: $G(\mathbf{I} - \mathbf{C})$ in SVUCM does not exactly match $G(\mathbf{C} - \mathbf{I})$ in SVTM, and the components of the two stress tensors can be quite larger for SVUCM than SVTM (although they both have similar variations around zero), see C_{xx} along $x = .5$ in Fig. 8. Second, the stationary solution seems determined by G only, and not by our Weissenberg number λ unlike the usual “creeping flow” solutions typically computed at fixed $\beta := \nu_s/(\nu_s + \nu_p) = .5$ with a “polymer viscosity” $\nu_p := G\lambda$.

Note however that the time-dependent numerical solutions of Fig. 8 are

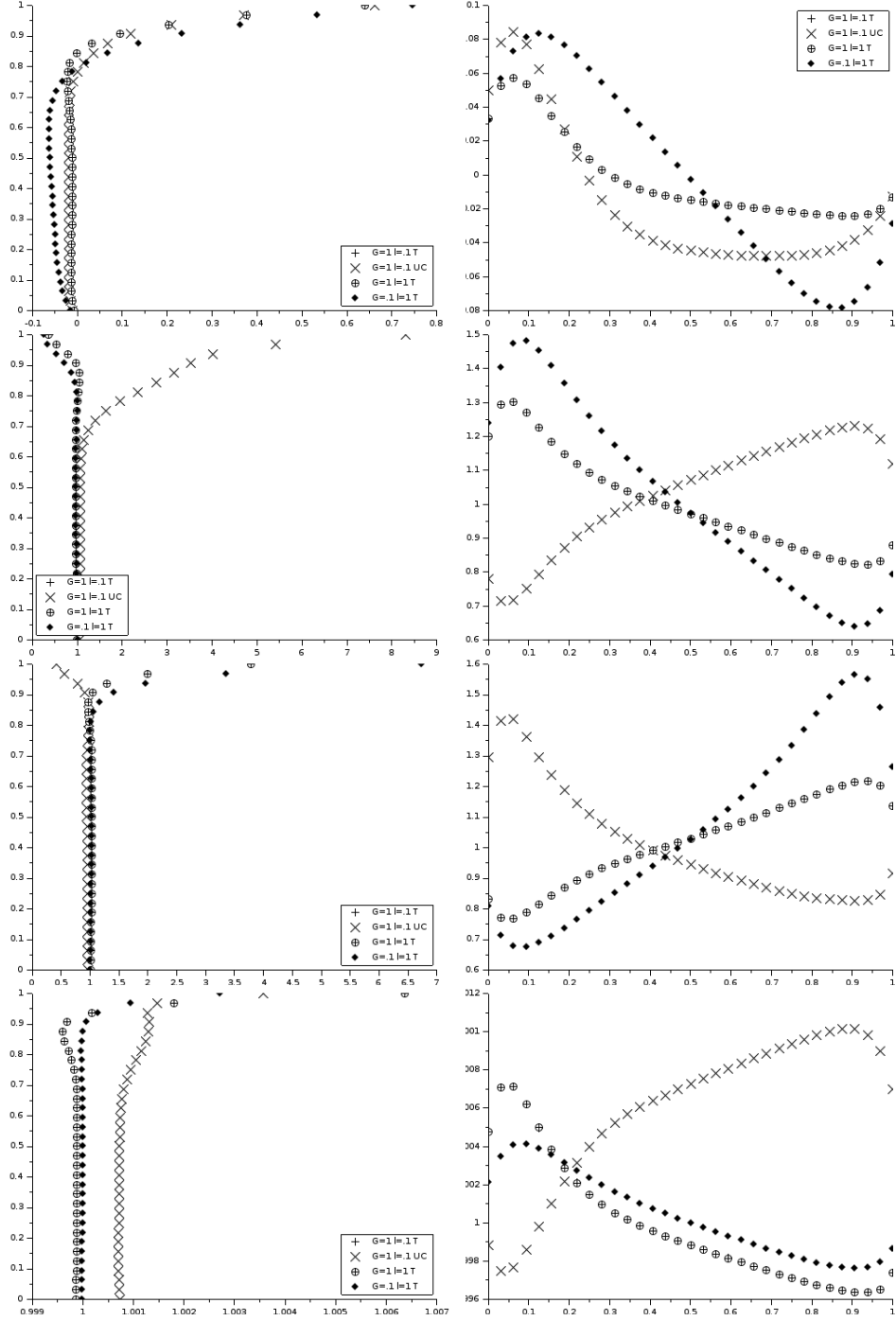


Figure 8: Lid-driven cavity at $g = 10^3$ with $\nu_s = .1$: cut $x = .5$ (left) and $y = .5$ (right). First line: U along $x = .5$ (left) and V along $y = .5$ (right), then c_{xx}, c_{yy}, c_{zz} (from second to fourth): for $G = .1, 1, \lambda = .1, 1$, SVTM (T) and SVUCM (UC).

quickly stationary in time for the smallest value $G = .1$, and seem limited in accuracy due to the presence of viscosity. In Fig. 10, we refine the mesh to $65 \times 65 = 4225$ cells: the ℓ^1 norm of the differences between two successive solutions as a function of time (our stationarity criterium) stagnates at a higher level, a plateau which is the same for all values of G smaller than .1 (see Fig. 9 for the converged solutions when $G = 10^{-1}$ and $G = 10^{-10}$). So our numerical experiment seems actually interesting only for large enough values of G , when shearing becomes more difficult and when strain is not so large (see the variations of U and V with G in Fig. 8).

Now, for larger G , we do observe convergence in time to stationary states without reaching a plateau both for SVTM and SVUCM. However, SVTM and SVUCM solutions now strongly differ. Solutions to SVT and SVUCM almost coincide at $\nu_s = .1$ and $G = 1$ and this is easily seen from the velocity vector fields $\mathbf{U} = (U, V)$ (see e.g. Fig. 11). Then, if we increase G to 10, large-time SVTM simulations seem to converge (in time and space) to solutions with only one main vortex, which is only slightly deformed and influenced by ν_s, λ (see in Fig. 11). On the contrary, SVUCM converge to a different type of solution which is also captured when ν_s is smaller, see Fig. 12.

5 Conclusion

In this work, motivated by the need for better numerical models of viscoelastic flows, we first have derived new hyperbolic models in the framework of shallow free-surface flows proposed by Saint-Venant. This extends Saint-Venant 2D shallow-water model to Maxwell fluid and is a continuation of our 1D work [10].

One model coincides with the zero-retardation Oldroyd-B case which had been obtained somewhat differently in [11] (without a precise study of solutions like here). The other suggests one to use a viscoelastic equation for a conformation tensor with a time-rate different than what is usually done in the literature (i.e. the Gordon-Schowalter derivatives).

Next, we have also proposed Finite-Volume (FV) discretizations that preserve the essential properties of the new models: mass and momentum conservation, plus a free-energy dissipation. Numerical simulations have been performed with the FV schemes that phenomenologically prove the physical soundness of the model in simple free-shear flows.

Quantitative evaluations in the lid-driven cavity testcase also show the interest of the approach to investigate more realistic strongly-sheared viscoelastic flows. Our numerical scheme should however still be improved to better understand standard benchmarks with large strains (and then with a HWNP, quite often), where differences between the two models (SVTM and SVUCM) with two different time-rates may be important. In particular, accuracy should be improved in the low Froude regime. This will be the object of future work.

References

- [1] A. Afonso, P.J. Oliveira, F.T. Pinho, and M.A. Alves, *The log-conformation tensor approach in the finite-volume method framework*, Journal of Non-Newtonian Fluid Mechanics **157** (2009), no. 1–2, 55–65.

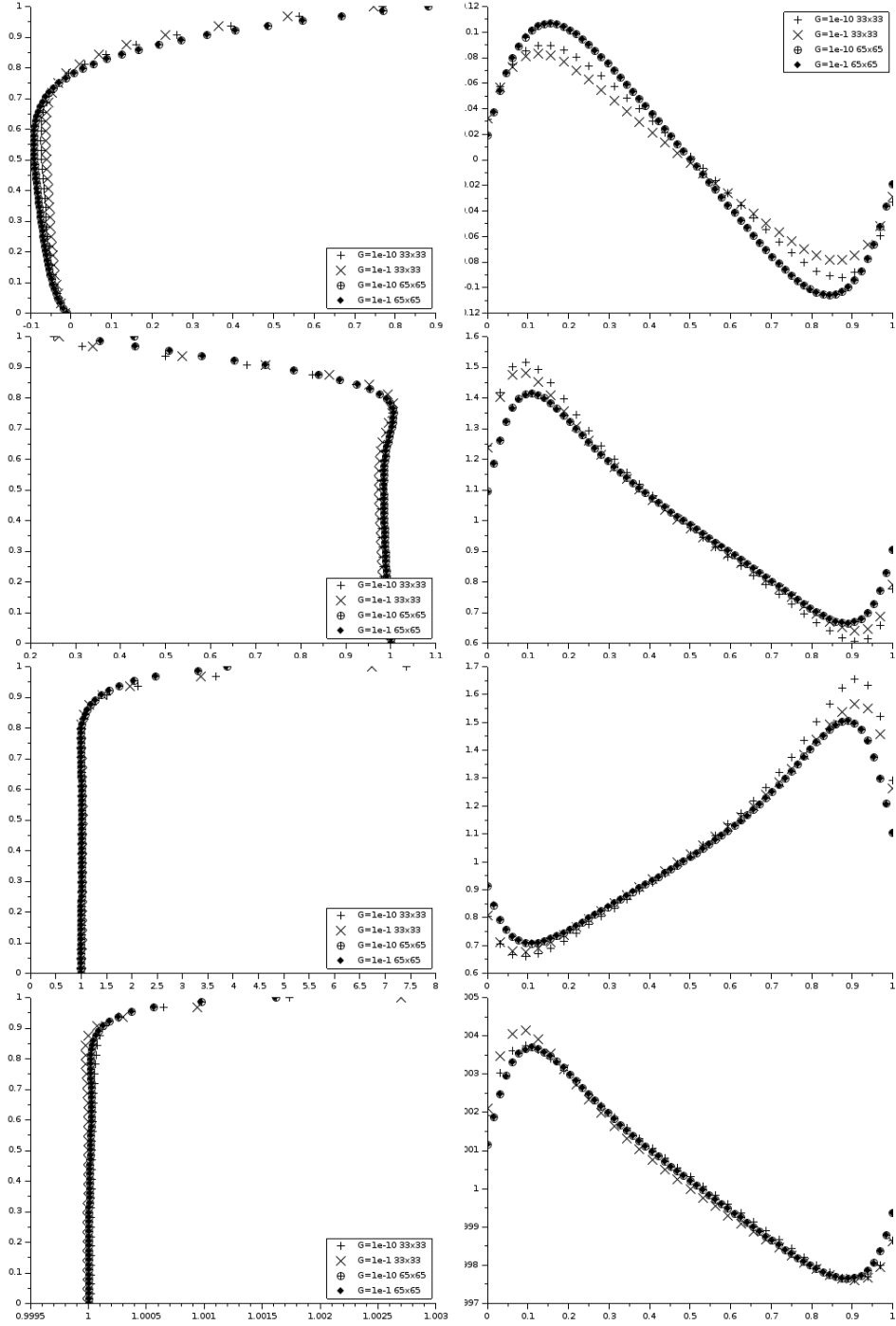


Figure 9: Lid-driven cavity at $g = 10^3$ with $\nu_s = .1$: cut $x = .5$ (left) and $y = .5$ (right). First line: U along $x = .5$ (left) and V along $y = .5$ (right), then c_{xx}, c_{yy}, c_{zz} (from second to fourth): for $\lambda = 1$, SVTM, $G = .1, 1^{-10}$ and two meshes.

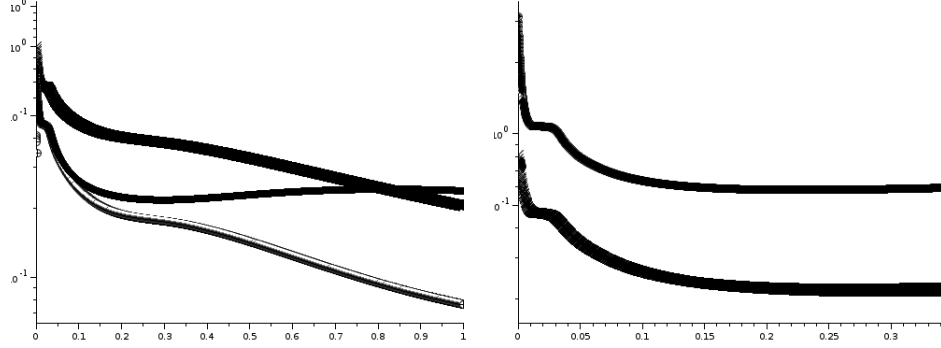


Figure 10: Lid-driven cavity at $g = 10^3$ with $\nu_s = .1$. Left: ℓ^1 norms of the differences between two successive solutions as a function of time (our stationarity criterium) for the four cases of Fig. 8 with $33 \times 33 = 1089$ cells, namely $G = 1, \lambda = .1$ UC then $G = .1, \lambda = 1$ T and $G = 1, \lambda = .1, 1$ T (superimposed) from top to bottom. Right: stagnation reaches a plateau higher with $65 \times 65 = 4225$ than with $33 \times 33 = 1089$ cells, for $G = 10^{-1}$ and $G = 10^{-10}$ (superimposed).

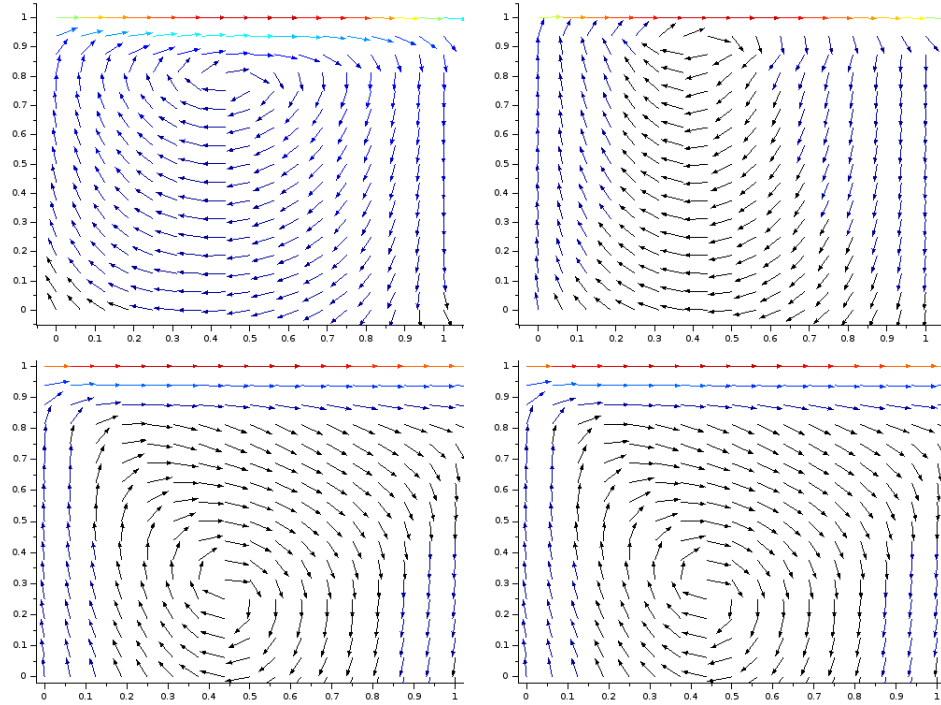


Figure 11: Lid-driven cavity at $g = 10^3$: SVTM velocity vector fields $\mathbf{U} = (U, V)$ at $T = 1$ for $\nu_s = .1, .01$ (left/right) and $G = 1, 10$ (top/bottom).

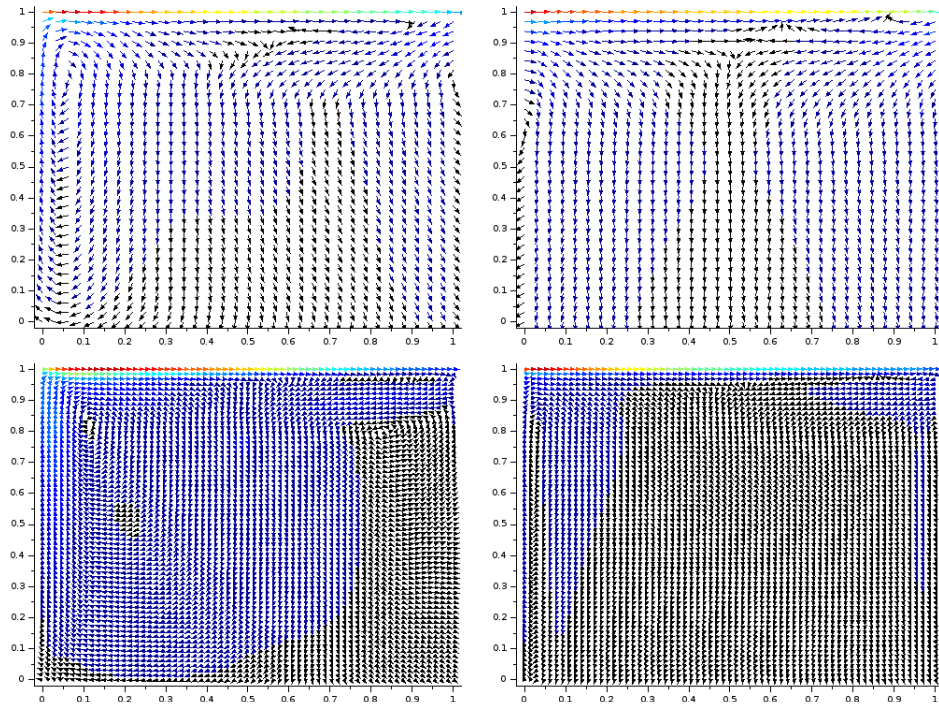


Figure 12: Lid-driven cavity at $g = 10^3$: SVUCM velocity vector field $\mathbf{U} = (U, V)$ at $33 \times 33 = 1089$ and $65 \times 65 = 4225$ points (top/bottom) for $G = 1, 10$ (left/right) and $\nu_s = 10^{-2}$, $\lambda = .1$.

- [2] J. W. Barrett and S. Boyaval, *Existence and approximation of a (regularized) Oldroyd-B model*, Tech. report, 2010, arXiv:0907.4066v2.
- [3] ———, *Existence and approximation of a (regularized) Oldroyd-B model*, M3AS **21** (2011), no. 9, 1783–1837.
- [4] John W Barrett and Sébastien Boyaval, *Finite-element approximation of the FENE-P model*, IMA Journal of Numerical Analysis (2017), in press, working paper arXiv:1704.00886 or preprint hal-01501197.
- [5] Christophe Berthon, Frédéric Coquel, and Philippe G. LeFloch, *Why many theories of shock waves are necessary: kinetic relations for non-conservative systems*, Proceedings of the Royal Society of Edinburgh: Section A Mathematics **142** (2012), 1–37.
- [6] Stefano Bianchini and Alberto Bressan, *Vanishing viscosity solutions of nonlinear hyperbolic systems*, Ann. of Math. (2) **161** (2005), no. 1, 223–342. MR 2150387 (2007i:35160)
- [7] R. B. Bird, C. F. Curtiss, R. C. Armstrong, and O. Hassager, *Dynamics of polymeric liquids*, vol. 1: Fluid Mechanics, John Wiley & Sons, New York, 1987.
- [8] R. Byron Bird and W. J. Drugan, *An exploration and further study of an enhanced oldroyd model*, Physics of Fluids **29** (2017), no. 5, 053103.
- [9] François Bouchut, *Nonlinear stability of finite volume methods for hyperbolic conservation laws and well-balanced schemes for sources*, Frontiers in Mathematics, Birkhäuser Verlag, Basel, 2004. MR MR2128209 (2005m:65002)
- [10] François Bouchut and Sébastien Boyaval, *A new model for shallow viscoelastic fluids*, M3AS **23** (2013), no. 08, 1479–1526.
- [11] François Bouchut and Sébastien Boyaval, *Unified derivation of thin-layer reduced models for shallow free-surface gravity flows of viscous fluids*, European Journal of Mechanics - B/Fluids **55**, Part 1 (2016), 116–131.
- [12] S. Boyaval, *Johnson-Segalman – Saint-Venant equations for viscoelastic shallow flows in the pure elastic limit*, Proceedings in Mathematics and Statistics (PROMS) of the International Conference on Hyperbolic Problems: Theory, Numeric and Applications in Aachen 2016 (C. Klingenberg and M. Westdickenberg, eds.), 2017.
- [13] Sébastien Boyaval, Tony Lelièvre, and Claude Mangoubi, *Free-energy-dissipative schemes for the Oldroyd-B model*, M2AN Math. Model. Numer. Anal. **43** (2009), no. 3, 523–561. MR 2536248 (2010k:65197)
- [14] Gui-Qiang Chen and Dehua Wang, *Chapter 5 the cauchy problem for the euler equations for compressible fluids*, Handbook of Mathematical Fluid Dynamics, vol. 1, North-Holland, 2002, pp. 421–543.
- [15] Elisabetta Chiodaroli, Camillo De Lellis, and Ondřej Kreml, *Global ill-posedness of the isentropic system of gas dynamics*, Communications on Pure and Applied Mathematics **68** (2015), no. 7, 1157–1190.

- [16] C. M. Dafermos, *Hyperbolic conservation laws in continuum physics*, vol. GM 325, Springer-Verlag, Berlin, 2000.
- [17] A.J.C. de Saint-Venant, *Théorie du mouvement non-permanent des eaux, avec application aux crues des rivières et à l'introduction des marées dans leur lit*, C. R. Acad. Sc. Paris **73** (1871), 147–154.
- [18] Brian J. Edwards and Antony N. Beris, *Remarks concerning compressible viscoelastic fluid models*, Journal of Non-Newtonian Fluid Mechanics **36** (1990), 411 – 417.
- [19] R. Fattal and R. Kupferman, *Time-dependent simulation of visco-elastic flows at high weissenberg number using the log-conformation representation*, J. Non-Newtonian Fluid Mech. **126** (2005), 23–27.
- [20] Gérard Gallice, *Schémas de type godunov entropiques et positifs préservant les discontinuités de contact*, Comptes Rendus de l'Académie des Sciences - Series I - Mathematics **331** (2000), no. 2, 149–152.
- [21] Sergey L. Gavriluk, Kseniya A. Ivanova, and Nicolas Favrie, *Multi-dimensional shear shallow water flows : problems and solutions*, (2017), working paper or preprint.
- [22] Jean-Frédéric Gerbeau and Benoît Perthame, *Derivation of viscous Saint-Venant system for laminar shallow water ; numerical validation*, Discrete and continuous dynamical system Series B **1** (2001), no. 1, 89–102.
- [23] Edwige Godlewski and Pierre-Arnaud Raviart, *Numerical approximation of hyperbolic systems of conservation laws*, Applied Mathematical Sciences, vol. 118, Springer-Verlag, New York, 1996. MR MR1410987 (98d:65109)
- [24] Amr Guaily, Eric Cheluget, Karen Lee, and Marcelo Epstein, *A new hyperbolic model and an experimental study for the flow of polymer melts in multi-pass rheometer*, Computers & Fluids **44** (2011), no. 1, 258 – 266.
- [25] Amr Guaily and Marcelo Epstein, *A unified hyperbolic model for viscoelastic liquids*, Mechanics Research Communications **37** (2010), no. 2, 158 – 163.
- [26] Kseniya A Ivanova, Sergey L Gavriluk, Boniface Nkonga, and Gael L. Richard, *Formation and coarsening of roll-waves in shear shallow water flows down an inclined rectangular channel*, (2016), working paper or preprint.
- [27] M.W. Johnson and D. Segalman, *A model for viscoelastic fluid behavior which allows non-affine deformation*, Journal of Non-Newtonian Fluid Mechanics **2** (1977), no. 3, 255 – 270.
- [28] Philipp Knechtges, Marek Behr, and Stefanie Elgeti, *Fully-implicit log-conformation formulation of constitutive laws*, Journal of Non-Newtonian Fluid Mechanics **214** (2014), no. 0, 78–87.
- [29] Randall J. LeVeque, *Finite volume methods for hyperbolic problems*, Cambridge Texts in Applied Mathematics, Cambridge University Press, Cambridge, 2002. MR MR1925043 (2003h:65001)

- [30] F. Marche, *Derivation of a new two-dimensional viscous shallow water model with varying topography, bottom friction and capillary effects*, European Journal of Mechanics-B/Fluids **26** (2007), no. 1, 49–63.
- [31] Nader Masmoudi, *Global existence of weak solutions to macroscopic models of polymeric flows*, Journal de Mathématiques Pures et Appliquées **96** (2011), no. 5, 502–520.
- [32] James Clerk Maxwell, *On the dynamical theory of gases*, Philosophical Transactions of the Royal Society of London **157** (1867), 49–88.
- [33] J. G. Oldroyd, *On the formulation of rheological equations of state*, Proceedings of the Royal Society of London. Series A. Mathematical and Physical Sciences **200** (1950), no. 1063, 523–541.
- [34] Hans Christian Öttinger, *Stochastic processes in polymeric fluids*, Springer-Verlag, Berlin, 1996. MR MR1383323 (97b:76008)
- [35] R. G. Owens and T. N. Philips, *Computational rheology*, Imperial College Press / World Scientific, 2002.
- [36] Tsorng-Whay Pan and Jian Hao, *Numerical simulation of a lid-driven cavity viscoelastic flow at high weissenberg numbers*, Comptes Rendus Mathématique **344** (2007), no. 4, 283 – 286.
- [37] Perrotti, Louis, Walkington, Noel J., and Wang, Daren, *Numerical approximation of viscoelastic fluids*, ESAIM: M2AN **51** (2017), no. 3, 1119–1144.
- [38] F.R. Phelan, M.F. Malone, and H.H. Winter, *A purely hyperbolic model for unsteady viscoelastic flow*, Journal of Non-Newtonian Fluid Mechanics **32** (1989), no. 2, 197 – 224.
- [39] M. Renardy, *Mathematical analysis of viscoelastic flows*, CBMS-NSF Conference Series in Applied Mathematics, vol. 73, SIAM, 2000.
- [40] Denis Serre, *Systèmes de lois de conservation. I*, Fondations. [Foundations], Diderot Editeur, Paris, 1996, Hyperbolicité, entropies, ondes de choc. [Hyperbolicity, entropies, shock waves]. MR 1459988 (99b:35139)
- [41] R.G. Sousa, R.J. Poole, A.M. Afonso, F.T. Pinho, P.J. Oliveira, A. Morozov, and M.A. Alves, *Lid-driven cavity flow of viscoelastic liquids*, Journal of Non-Newtonian Fluid Mechanics **234** (2016), 129 – 138.
- [42] J. J. Stoker, *Water waves: The mathematical theory with applications*, Interscience, London, 1957.
- [43] Ven te Chow, *Open-channel hydraulics*, Mc Graw Hill, 1959.
- [44] V. M. Teshukov, *Gas-dynamic analogy for vortex free-boundary flows*, Journal of Applied Mechanics and Technical Physics **48** (2007), no. 3, 303–309.
- [45] V.M. Teshukov, *Gas-dynamic analogy in the theory of stratified liquid flows with a free boundary*, Fluid Dynamics **42** (2007), no. 5, 807–817 (English).